THE JOURNAL OF BIOLOGICAL CHEMISTRY VOL. 291, NO. 38, pp. 20232–20246, September 16, 2016

S-Palmitoylation of a Novel Site in the β_2-Adrenergic Receptor Associated with a Novel Intracellular Itinerary*

Received for publication, March 9, 2016, and in revised form, July 29, 2016 Published, JBC Papers in Press, August 1, 2016, DOI 10.1074/jbc.M116.725762

Naoko Adachi[‡§1], Douglas T. Hess[‡§], Precious McLaughlin[‡§], and Jonathan S. Stamler[‡§¶2]

From the [‡]Institute for Transformative Molecular Medicine, Case Western Reserve University School of Medicine and University Hospitals Case Medical Center, Cleveland, Ohio 44106, the [§]Department of Medicine, Case Western Reserve University School of Medicine, Cleveland, Ohio 44106, and the [¶]Harrington Discovery Institute, University Hospitals Case Medical Center, Cleveland, Ohio 44106

We report here that a population of human β_2-adrenergic receptors (β_2AR), a canonical G protein-coupled receptor, traffics along a previously undescribed intracellular itinerary via the Golgi complex that is associated with the sequential *S*-palmitoylation and depalmitoylation of a previously undescribed site of modification, Cys-265 within the third intracellular loop. Basal *S*-palmitoylation of Cys-265 is negligible, but agonist-induced β_2AR activation results in enhanced *S*-palmitoylation, which requires phosphorylation by the cAMP-dependent protein kinase of Ser-261/Ser-262. Agonist-induced turnover of palmitate occurs predominantly on Cys-265. Cys-265 *S*-palmitoylation is mediated by the Golgi-resident palmitoyl transferases zDHHC9/14/18 and is followed by depalmitoylation by the plasma membrane-localized acyl-protein thioesterase APT1. Inhibition of depalmitoylation reveals that *S*-palmitoylation of Cys-265 may stabilize the receptor at the plasma membrane. In addition, β_2AR *S*-palmitoylated at Cys-265 are selectively preserved under a sustained adrenergic stimulation, which results in the down-regulation and degradation of βAR. Cys-265 is not conserved in β_1AR, and *S*-palmitoylation of Cys-265 may thus be associated with functional differences between β_2AR and β_1AR, including relative resistance of β_2AR to down-regulation in multiple pathophysiologies. Trafficking via the Golgi complex may underlie new roles in G protein-coupled receptor biology.

The function of G protein-coupled receptors (GPCR)[3] is regulated by diverse posttranslational modifications, which in the case of the canonical GPCR, the β_2-adrenergic receptor (β_2AR), include prominent phosphorylation and *S*-palmitoylation. The dynamic regulation of individual posttranslational modifications and potential cross-talk between them remain incompletely understood. A number of GPCR have been shown to be *S*-palmitoylated at 1–3 Cys residues located within the C-terminal tail at the cytoplasmic end of the seventh transmembrane segment (1). The first example of *S*-palmitoylation of a ligand-activated GPCR (following the seminal demonstration of *S*-palmitoylation of the light-activated photoreceptor GPCR rhodopsin (2)) was provided by the β_2AR. Metabolic labeling with [^{3}H]palmitic acid in combination with mutational analysis revealed that the β_2AR incorporates palmitate at Cys-341 (numbering here and below is according to the human sequence) within the C-terminal cytoplasmic tail under basal conditions (3), and it was subsequently suggested that agonist stimulation increases the rate of palmitate turnover (4). It is also reported that mutation of Cys-341 inhibits coupling of the β_2AR to G_s (3) and suppresses agonist-induced recruitment of β-arrestin (5), although the extent to which those effects of mutation reflect an absence of palmitoylation *per se* has not been determined.

In the 27 years following the initial report (3), it has been assumed that Cys-341 represents the sole site of *S*-palmitoylation within the β_2AR, consistent with elimination of metabolic labeling with [^{3}H]palmitic acid under basal conditions by mutation of Cys-341 (3). We report here the discovery of a second site of β_2AR *S*-palmitoylation, at Cys-265 within the third intracellular loop. *S*-Palmitoylation of Cys-265 is predominantly dependent upon agonist activation of the β_2AR and requires both phosphorylation by cAMP-dependent kinase (PKA) of Ser-261/Ser-262 and receptor internalization. *S*-Palmitoylation of Cys-265 is rapidly reversed upon withdrawal of agonist. Agonist-induced turnover of palmitate on the β_2AR occurs predominantly on Cys-265. We identified the enzymes responsible for *S*-palmitoylation of Cys-265 as zDHHC9/14/18, which constitute a distinct subfamily of the 23 mammalian zDHHC defined by phylogenetic tree analysis, and we identified the enzyme responsible at least in large part for depalmitoylation as the plasma membrane-localized acyl-protein thioesterase 1 (APT1). zDHHC9/14/18 reside in the Golgi/trans-Golgi subcellular compartment (Golgi complex), and trafficking of the β_2AR to the Golgi complex for *S*-palmitoylation and thence to the plasma membrane for depalmitoylation represents a previously unreported intracellular itinerary for the β_2AR initiated by agonist stimulation. Inhibition of depalmitoylation revealed that *S*-palmitoylation of Cys-265 stabilizes the receptor at the

* This work was supported in part by National Institutes of Health Grant P01HL075443. The authors declare that they have no conflicts of interest with the contents of this article. The content is solely the responsibility of the authors and does not necessarily represent the official views of the National Institutes of Health.

[1] Current address: Biosignal Research Center, Kobe University, Kobe, Japan 657-8501.

[2] To whom correspondence should be addressed: Institute for Transformative Molecular Medicine, Case Western Reserve University, 10900 Euclid Ave., Location Code 7294, Cleveland, OH 44106. Tel.: 216-368-5725; E-mail: jonathan.stamler@case.edu.

[3] The abbreviations used are: GPCR, G protein-coupled receptor; βAR, β-adrenergic receptor; APT1, acyl-protein thioesterase 1; acyl-RAC, resin-assisted capture of fatty acylated proteins; IBMX, 3-isobutyl-1-methylxanthine; ISO, isoproterenol; 2-BP, 2-bromopalmitate; PROP, isoproterenol; PalmB, palmostatin B; qPCR, quantitative reverse-transcription PCR; ANOVA, analysis of variance.

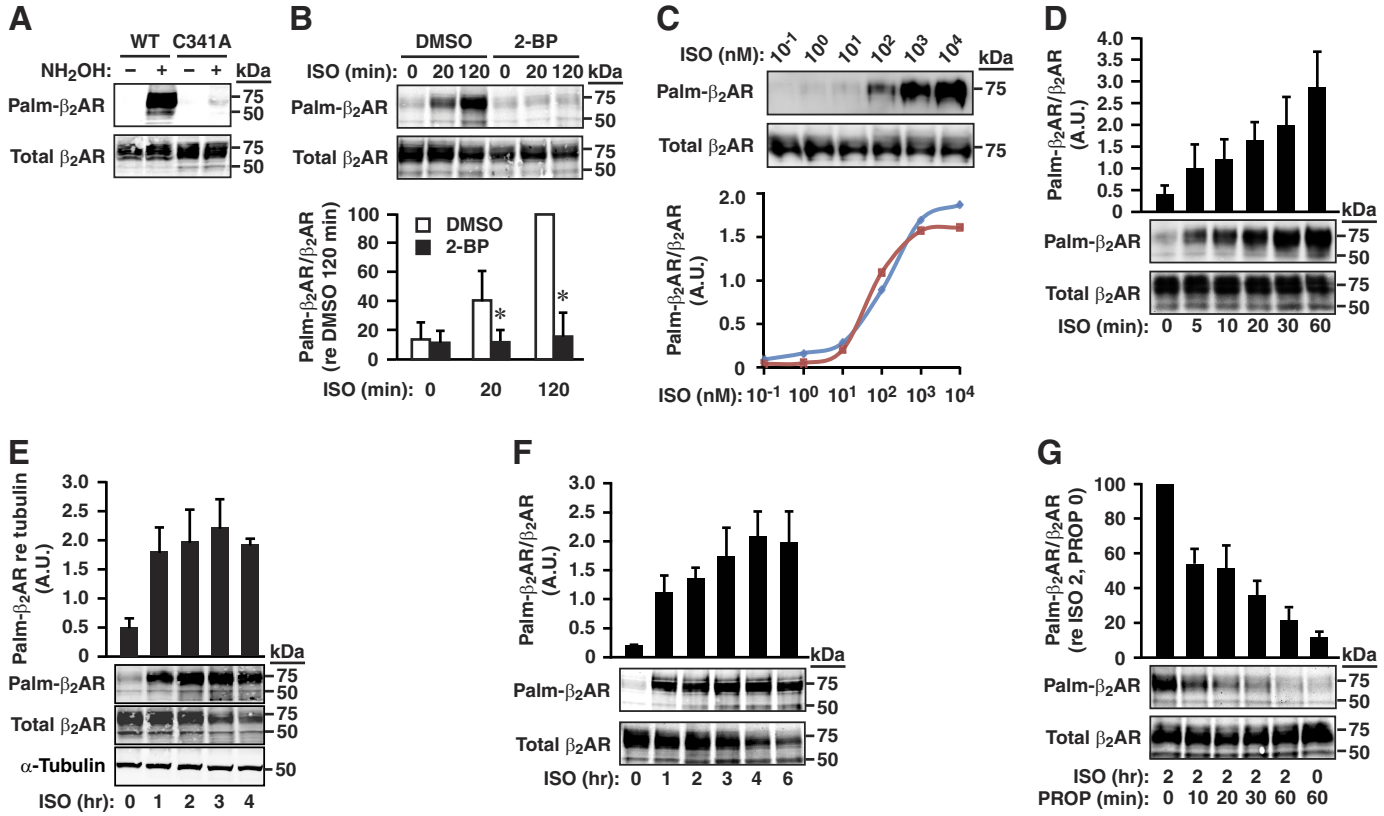

FIGURE 1. **Ligand-induced *S*-palmitoylation of a second site(s) within the β_2AR.** *A*, as shown by acyl-RAC, basal *S*-palmitoylation of the wild-type β_2AR is greatly but not completely diminished by mutation of Cys-341. Omission of NH_2OH (0.5 M) serves as a control for specificity of the acyl-RAC procedure regarding palmitoylation. *B*, *S*-palmitoylation of β_2AR-C341A is induced in a time-dependent fashion during ligand-induced activation by ISO (10 μM), and the signal detected with acyl-RAC is eliminated by the inhibitor of *S*-palmitoylation, 2-BP (100 μM, 1 h). DMSO, vehicle control. $n = 6$; *, $p < 0.05$. *C*, dose dependence of ISO-induced *S*-palmitoylation of β_2AR-C341A as assessed by acyl-RAC. ISO was applied for 1 h at the indicated doses followed by acyl-RAC (*top*) and quantification of the results of two separate experiments (*bottom*). *A.U.*, arbitrary unit. *D*, ISO-induced *S*-palmitoylation of β_2AR-C341A increases linearly over a time course of 1 h. $n = 3$. *E*, ISO-induced *S*-palmitoylation of β_2AR-C341A plateaus after 1 h, and the abundance of *S*-palmitoylated receptor is maintained for at least 4 h, whereas absolute levels of receptor (*Total β_2AR*) are diminished. $n = 3$; no significant differences between any time points after 0 h by ANOVA ($p > 0.05$). *F*, the proportion of *S*-palmitoylated β_2AR-C341A increases with maintained ISO stimulation to reach a plateau at 4 h, as a result of the fact that the population of *S*-palmitoylated receptors remains unchanged, whereas the total pool of receptors diminishes. $n = 3$. *G*, upon removal of ISO (10 μM, 2 h) and the addition of PROP (100 μM) to terminate receptor activation, *S*-palmitoylation of β_2AR-C341A declines with $t_{1/2} \sim 17$ min. $n = 6$.

membrane. Further, we found that under conditions of sustained adrenergic stimulation (as in pathophysiologies that may result in down-regulation of βAR), the β_2AR *S*-palmitoylated at Cys-265 are selectively preserved, maintaining a pool of receptors that are primed for reactivation upon depalmitoylation.

Results

Agonist-induced and Dynamic S-Palmitoylation of a Second Site(s) within the β_2AR—To examine β_2AR *S*-palmitoylation, we employed the acyl-RAC method (resin-assisted capture of fatty acylated proteins) in which the thioester bond between palmitate and Cys is cleaved with neutral hydroxylamine and the resultant free thiol is coupled to thiopropyl-Sepharose for pulldown and subsequent analysis (6, 7). This method directly assesses the presence of palmitate-modified Cys, and omission of hydroxylamine provides a rigorous control for false positives. In human embryonic kidney (HEK293) cells stably expressing FLAG-tagged wild-type human β_2AR, acyl-RAC in combination with Western blotting for FLAG revealed *S*-palmitoylation under basal conditions (Fig. 1*A*), consistent with previous results obtained with metabolic labeling by [^{3}H]palmitic acid (3, 4). The acyl-RAC assay cannot by itself distinguish between one or more sites of *S*-palmitoylation within a given substrate. In HEK293 cells stably expressing FLAG-tagged β_2AR in which Cys-341 was mutated to Ala (β_2AR-C341A), *S*-palmitoylation of β_2AR under basal conditions was greatly diminished, but we consistently observed a small, hydroxylamine-dependent signal (Fig. 1*A*), suggesting the possibility of an additional site(s) of *S*-palmitoylation. Because previous results suggested that agonist-induced activation resulted in the turnover of palmitate on the β_2AR (4), we examined the effects of activation of β_2AR-C341A by the prototypical β_2AR agonist isoproterenol (ISO). Stimulation with ISO (10 μM) greatly enhanced *S*-palmitoylation of β_2AR-C341A (Fig. 1*B*). Enhancement of *S*-palmitoylation was evident following stimulation with 1 nM ISO, and a sigmoidal dose-response curve revealed progressive enhancement through 10 μM ISO (Fig. 1*C*); 10 μM ISO was employed in most subsequent assays. The fidelity of the acyl-RAC method as a reporter of *S*-palmitoylation under these conditions was verified by the finding that treatment with the inhibitor of *S*-palmitoylation, 2-bromopalmitate (2-BP, 100 μM), largely eliminated hydroxylamine-dependent pulldown of β_2AR-C341A following stimulation with ISO (Fig. 1*B*). Thus, there is a second

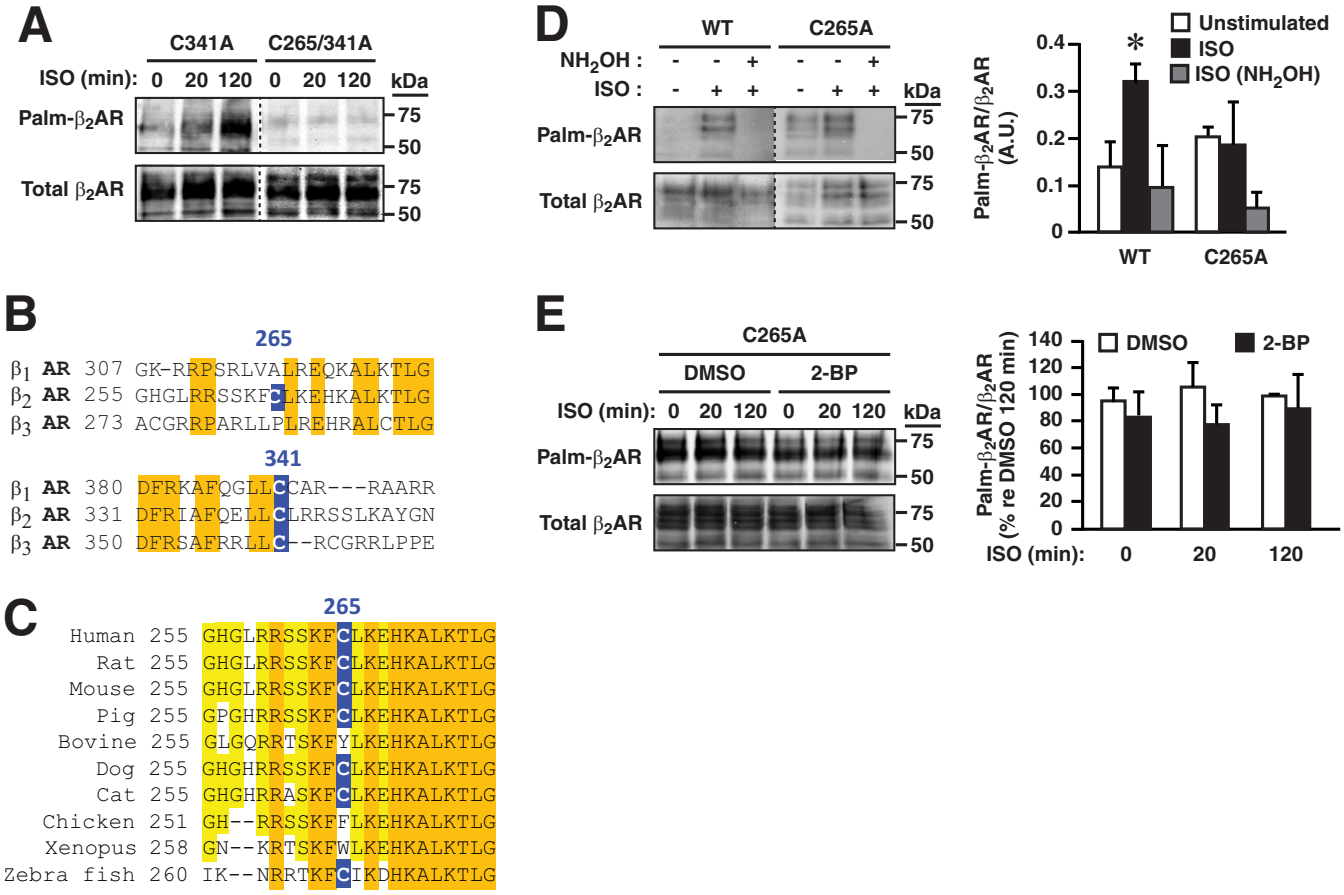

FIGURE 2. **Cys-265 is the second site of *S*-palmitoylation within the β_2AR.** *A*, combined mutation of Cys-341 and Cys-265 eliminates ISO-induced (10 μM) *S*-palmitoylation of β_2AR as assessed by acyl-RAC. *B*, Cys-265 is not conserved in β_1AR or β_3AR (human). *C*, conservation of Cys-265 across phylogeny. Cys-341 is conserved in all species listed. *D*, mutation of Cys-265 eliminates ISO-induced (10 μM) metabolic labeling of the β_2AR by 17-octadecynoic acid as detected by bio-orthogonal click chemistry. Elimination of labeling by treatment with neutral hydroxylamine (NH_2OH, 1 M, 1 h) verifies thioester linkage. Data are presented as mean ± S.D.; $n = 3$. *, $p < 0.05$ *versus* unstimulated and ISO plus NH_2OH WT by ANOVA. *A.U.*, arbitrary unit. *E*, whereas 2-BP (100 μM, 1-h pretreatment) eliminates ISO-induced *S*-palmitoylation of β_2AR-C341A (shown in Fig. 1*B*), neither ISO stimulation nor 2-BP affects *S*-palmitoylation of β_2AR-C265A, verifying Cys-265 as the predominant site of dynamic *S*-palmitoylation within the β_2AR. DMSO = vehicle control. Data are presented as mean ± S.D.; $n = 3$. No significant differences by ANOVA ($p > 0.05$).

site(s) of *S*-palmitoylation within the β_2AR, and *S*-palmitoylation of that site(s) is predominantly dependent upon receptor activation.

Enhanced *S*-palmitoylation of β_2AR-C341A was evident as soon as 5 min after exposure to ISO, and the population stoichiometry of S-palmitoylation increased linearly until it reached a plateau after 1 h of stimulation (Fig. 1, *D* and *E*). Quantification of Western blotting analysis following acyl-RAC revealed that the proportion of β_2AR modified by *S*-palmitoylation of Cys-265 plateaued at about 25%. It has been shown that sustained activation of the β_2AR results in β_2AR down-regulation, which reflects at least in part β_2AR ubiquitination by Mdm2 (mouse double minute 2 homolog) (8). We observed that β_2AR-C341A was down-regulated with prolonged stimulation (>2 h) by ISO but that the abundance of *S*-palmitoylated β_2AR was not decreased (Fig. 1, *E* and *F*). Thus, the population of β_2AR that is *S*-palmitoylated at the second site(s) is apparently distinct from the population that is subject to ubiquitination, and further, down-regulation accompanying prolonged stimulation of β_2AR results in a progressive and substantial (~85%) increase in the proportion (relative abundance) of β_2AR that is *S*-palmitoylated at the second site(s) (Fig. 1*F*).

Gradual acquisition of a steady state of *S*-palmitoylation while maintaining stimulation by ISO points to establishment of an equilibrium between S-palmitoylation and depalmitoylation. Active depalmitoylation was indicated by the finding that removal of ISO (following exposure for 2 h), coupled with the addition of the β_2AR antagonist propranolol (PROP, 100 μM) to assure truncation of receptor activation, was followed by rapid loss of palmitate from β_2AR-C341A as revealed by acyl-RAC ($t_{1/2} = 17.65$ min) (Fig. 1*G*).

Cys-265 Is the Second Site of β_2AR S-Palmitoylation—To identify the site(s) of agonist-induced palmitoylation, Cys residues within the β_2AR were mutated to Ala, and mutant or wild-type receptors were stably expressed in HEK293 cells. Whereas mutation of the canonical site of *S*-palmitoylation, Cys-341, had no apparent effect on ISO-induced *S*-palmitoylation as assessed by acyl-RAC, the combined mutation of Cys-341 and of Cys-265 within the third intracellular loop largely eliminated agonist-induced *S*-palmitoylation (Fig. 2*A*). Thus, Cys-265 is the single second site of *S*-palmitoylation. Unlike Cys-341, the canonical C-terminal-tail site of palmitoylation, Cys-265, is not conserved in β_1AR or β_3AR (Fig. 2*B*) and is conserved within β_2AR more variably across vertebrate phylogeny than Cys-341 (Fig. 2*C*).

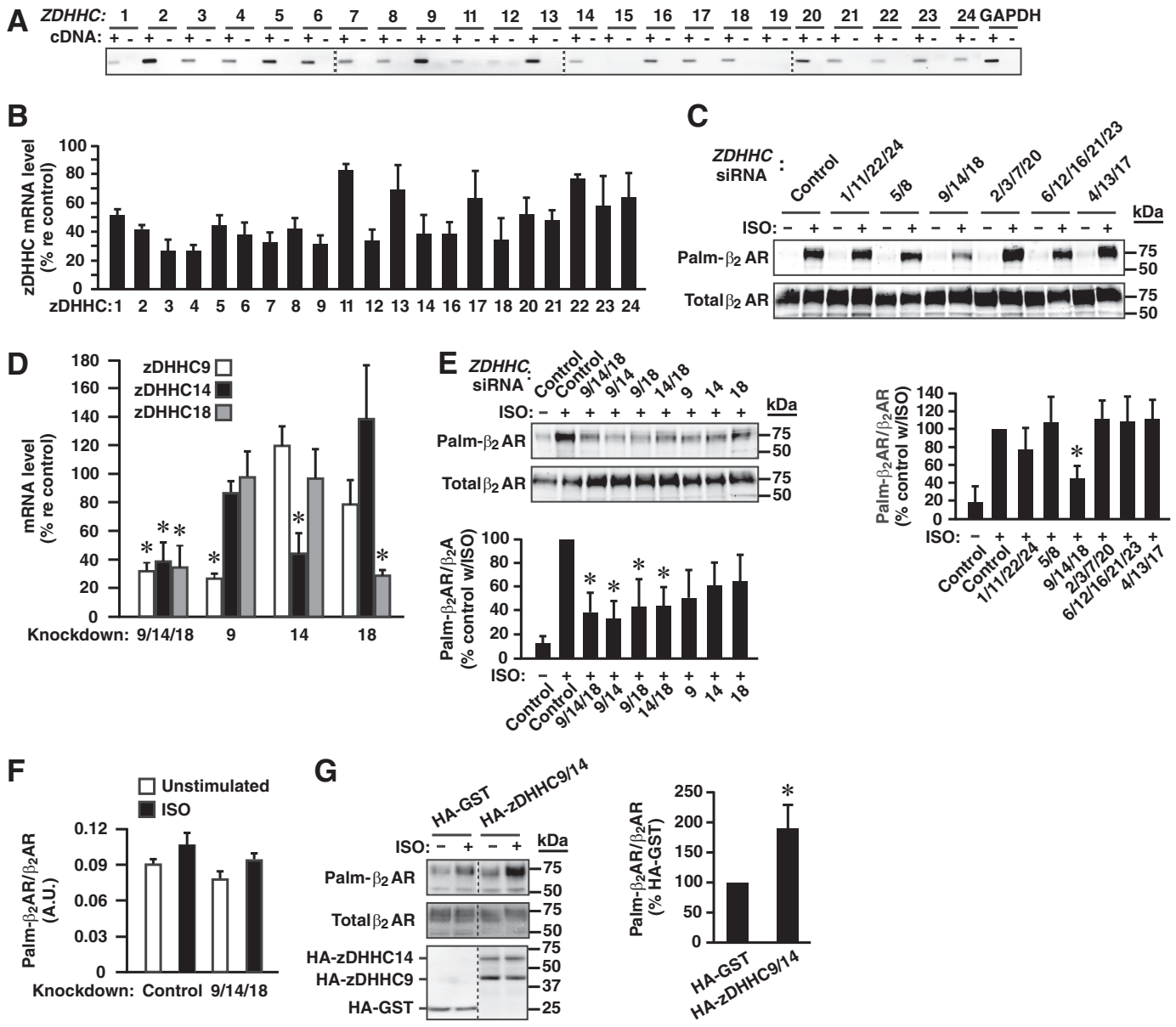

FIGURE 3. **β_2AR Cys-265 is *S*-palmitoylated by zDHHC9/14/18.** *A*, analysis by qPCR demonstrates that 21 of 23 zDHHC are expressed in HEK293 cells. *B*, knockdown of individual zDHHC with siRNA. *C*, in HEK293 cells expressing β_2AR-C341A, knockdown by siRNA of the six separate zDHHC families comprising all human DHHC indicates that zDHHC9/14/18 are predominantly responsible for the *S*-palmitoylation of β_2AR Cys-265 as assessed by acyl-RAC following stimulation with ISO (10 μM, 1 h). $n = 3$; *, $p < 0.05$ *versus* Control siRNA treated with ISO (ANOVA). *D*, knockdown of zDHHC9/14/18 individually and in combination. $n = 3$; *, $p < 0.05$ *versus* control siRNA (100%). *E*, knockdown by siRNA of zDHHC9, -14, and -18 individually and in combination demonstrates that zDHHC9/14/18 redundantly mediate *S*-pamitoylation of β_2AR Cys-265. $n = 3$; *, $p < 0.05$ *versus* control siRNA treated with ISO (10 μM, 1 h) (ANOVA). *F*, knockdown of zDHHC9/1/4/18 had no effect on *S*-palmitoylation of β_2AR-C265A (*i.e.* had no effect on *S*-palmitoylation of Cys-341). $n = 3$; no significant differences *versus* control siRNA. *A.U.*, arbitrary unit. *G*, transfection-induced expression of HA-tagged zDHHC9/14 results in enhanced ISO-induced *S*-palmitoylation of β_2AR Cys-265; transfection with HA-tagged GST served as control. $n = 3$; *, $p < 0.05$ *versus* control transfection.

We then examined agonist-induced turnover of palmitate on the wild type and β_2AR-C265A employing metabolic labeling with the ω-alkynyl-palmitate analog 17-octadecynoic acid followed by bio-orthogonal click chemistry with azide-PEG3-biotin (9–11). Treatment with ISO resulted in enhanced incorporation of 17-octadecynoic acid into the wild type but not β_2AR-C265A (Fig. 2*D*). In addition, whereas exposure to 2-BP largely eliminated ligand-induced *S*-palmitoylation of β_2AR-C341A following stimulation with ISO as assessed by acyl-RAC (Fig. 1*B*), 2-BP had no significant effect on *S*-palmitoylation of β_2AR-C265A (Fig. 2*E*). Thus, *S*-palmitoylation of Cys-265 apparently accounts for at least the large part of ligand-induced dynamic turnover of palmitate on the β_2AR, whereas *S*-palmitoylation of Cys-341 is relatively stable.

Cys-265 Is S-Palmitoylated by zDHHC9/14/18—In mammalian cells, enzymatic *S*-palmitoylation is mediated by a family of palmitoyl transferases comprising 23 enzymes that share a zinc-finger motif and an Asp-His-His-Cys active site configuration (zDHHC) (12, 13). Quantitative reverse-transcription PCR (qPCR) in HEK293 cells detected expression of all human *ZDHHC* except *ZDHHC15* and *ZDHHC19* (*ZDDHC10* is not expressed in human cells) (Fig. 3*A*). In HEK293 cells stably

expressing β_2AR-C341A, we employed siRNA-mediated knockdown to identify the zDHHC responsible for *S*-palmitoylation of Cys-265. We knocked down the 20 *ZDHHC* present in HEK293 cells in six sets that represent subfamilies as defined by phylogenetic tree analysis (13) and verified knockdown efficacy by qPCR (Fig. 3*B*). We found that knockdown of the subfamily of zDHHC comprising zDHHC9, zDHHC14, and zDHHC18 greatly diminished ISO-induced (10 μM, 1 h) *S*-palmitoylation of Cys-265, whereas knockdown of other subfamilies of zDHHC had no effect (Fig. 3*C*). Although individual knockdown of zDHHC9, zDHHC14, or zDHHC18 diminished *S*-palmitoylation of Cys-265, knockdown of zDHHC9/14, zDHHC9/18, or zDHHC14/18 had a larger effect (Fig. 3, *D* and *E*). In contrast, knockdown of zDHHC9/14/18 had no significant effect on the palmitoylation of Cys-341 (*i.e.* on palmitoylation of β_2AR-C265A (Fig. 3*F*)). In addition, overexpression of zDHHC9/14 in HEK293 cells expressing β_2AR-C341A significantly enhanced ISO-induced *S*-palmitoylation of Cys-265 (Fig. 3*G*). Thus, zDHHC9, zDHHC14, and zDHHC18, exclusively among the identified DHHC, redundantly mediated agonist-induced *S*-palmitoylation of Cys-265, and zDHHC9/14/18 did not address Cys-341.

Cys-265 Is Depalmitoylated by APT1—Agonist-induced *S*-palmitoylation of Cys-265 within the β_2AR is rapidly reversed upon removal of agonist (Fig. 1*G*), indicating the operation of a depalmitoylating mechanism. In mammalian cells, four thioesterases are well established as mediators of enzymatic depalmitoylation. The palmitoyl-protein thioesterases PPT1 (14, 15) and PPT2 (16) operate at the lysosome, whereas the acyl-protein thioesterases APT1 (17) and APT2 (18), members of the serine hydrolase/lysophospholipase family that share a Ser/His/Asp catalytic triad, have a broad subcellular distribution and are themselves *S*-palmitoylated and thereby localized to membranes including the plasma membrane (19). APT1/2 are therefore poised to mediate dynamic depalmitoylation in the context of cellular signaling, although the substrate specificities and regulation of APT1/2 are not well understood. We found by qPCR that all four protein thioesterases were expressed in HEK293 cells (Fig. 4*A*). To identify the enzyme(s) responsible for depalmitoylation of Cys-265, we first examined the effect of palmostatin B (PalmB), a catalytic inhibitor of APT1/2. We found that PalmB inhibited depalmitoylation of Cys-265 in β_2AR-C341A in a dose-dependent fashion after the termination of ISO-induced receptor activation (Fig. 4*B*), indicating that APT1 and/or APT2 mediated the depalmitoylation of Cys-265. We then employed siRNA-mediated knockdown of individual enzymes to isolate the activity responsible for depalmitoylation of Cys-265 as verified by qPCR (Fig. 4*C*) and determined that knockdown of APT1 suppressed the depalmitoylation, whereas knockdown of APT2, PPT1, or PPT2 had no significant effect (Fig. 4*D*). Thus, APT1 mediates depalmitoylation of Cys-265 within the β_2AR. However, it has recently been reported that additional members of the serine hydrolase enzyme superfamily exhibit PalmB-inhibitable protein depalmitoylating activity (20), and our results do not rule out a role for additional depalmitoylating enzymes in the regulation of Cys-265 *S*-palmitoylation. Confocal immunofluorescence microscopy of overexpressed but untagged APT1 demonstrated that, under these conditions, APT1 was localized predominantly to the plasma membrane (Fig. 4*E*); in contrast to zDHHC9/14/18 (see below), we did not observe a perinuclear concentration that would suggest localization of APT1 to the Golgi complex.

S-Palmitoylation of Cys-265 within the β_2AR Is Associated with a Previously Undescribed Intracellular Itinerary—The zDHHC palmitoyl transferases are integral membrane proteins that are associated with internal membranes as well as the plasma membrane, and it has been shown that zDHHC9/14/18 are localized to the Golgi complex (21, 22). It is well established that activation of β_2AR is followed by internalization and routing of the receptor into trafficking pathways that involve its association with endosomes, which may be followed by recycling to the plasma membrane or either proteasomal or lysosomal degradation (23). In view of the known subcellular localization of zDHHC9/14/18 to the Golgi complex, our results suggest the possibility that a population of the β_2AR traffics to the Golgi complex following agonist-induced internalization, which is followed by a return to the plasma membrane that would be required for depalmitoylation by plasma membrane-resident APT1, thus representing a previously undescribed intracellular itinerary for this receptor.

To examine this possibility, we employed confocal immunofluorescence microscopic analysis in HEK293 cells stably expressing FLAG-tagged wild-type β_2AR and transiently transfected with HA-tagged zDHHC9, -14, or -18. Under basal conditions, β_2AR (FLAG) immunofluorescence was localized to the plasma membrane, whereas zDHHC9 (HA) immunofluorescence was localized to the Golgi complex, as demonstrated by co-localization with the Golgi complex marker Golgi-RFP (Fig. 5*A*). Following stimulation with ISO (10 μM, 1 h), β_2AR immunofluorescence was observed in a perinuclear distribution where it co-localized with zDHHC9/14/18 immunofluorescence, consistent with localization to the Golgi complex (Fig. 5*B*). Labeling of FLAG-tagged β_2AR with anti-FLAG Ab prior to ISO stimulation directly demonstrated trafficking of plasma membrane-localized β_2AR to the Golgi complex, identified by Golgi-RFP ("antibody feeding" assay) (Fig. 5*C*). Disruption of the Golgi complex with brefeldin A (2 h) resulted in a dose-dependent decrease in subsequent ISO-induced (10 μM, 1 h) *S*-palmitoylation of Cys-265 within β_2AR-C341A (Fig. 5*D*), which was associated with delocalization of zDHHC9/14/18 from a perinuclear concentration to a diffuse cytoplasmic distribution (Fig. 5*E*). Thus, a population of the β_2AR traffics to the Golgi complex upon ligand-induced activation and internalization, where they are *S*-palmitoylated by zDHHC9/14/18 and from whence they must traffic to the plasma membrane for depalmitoylation by plasma membrane-localized APT1.

We also determined, by employing cell-surface biotin labeling followed by acyl-RAC, pulldown of biotinylated proteins with streptavidin, and Western blotting for the β_2AR, that at least some proportion of the β_2AR *S*-palmitoylated at Cys-265 following ISO stimulation (10 μM, 1 h) is localized to the plasma membrane following transit from the Golgi complex (Fig. 5*F*).

PKA-mediated Phosphorylation of Ser-261/Ser-262 Is Necessary but Not Sufficient for Cys-265 S-Palmitoylation—Ligand-induced activation of the β_2AR activates G_s and thereby adenylyl cyclase, which generates cAMP, thus activating PKA. PKA

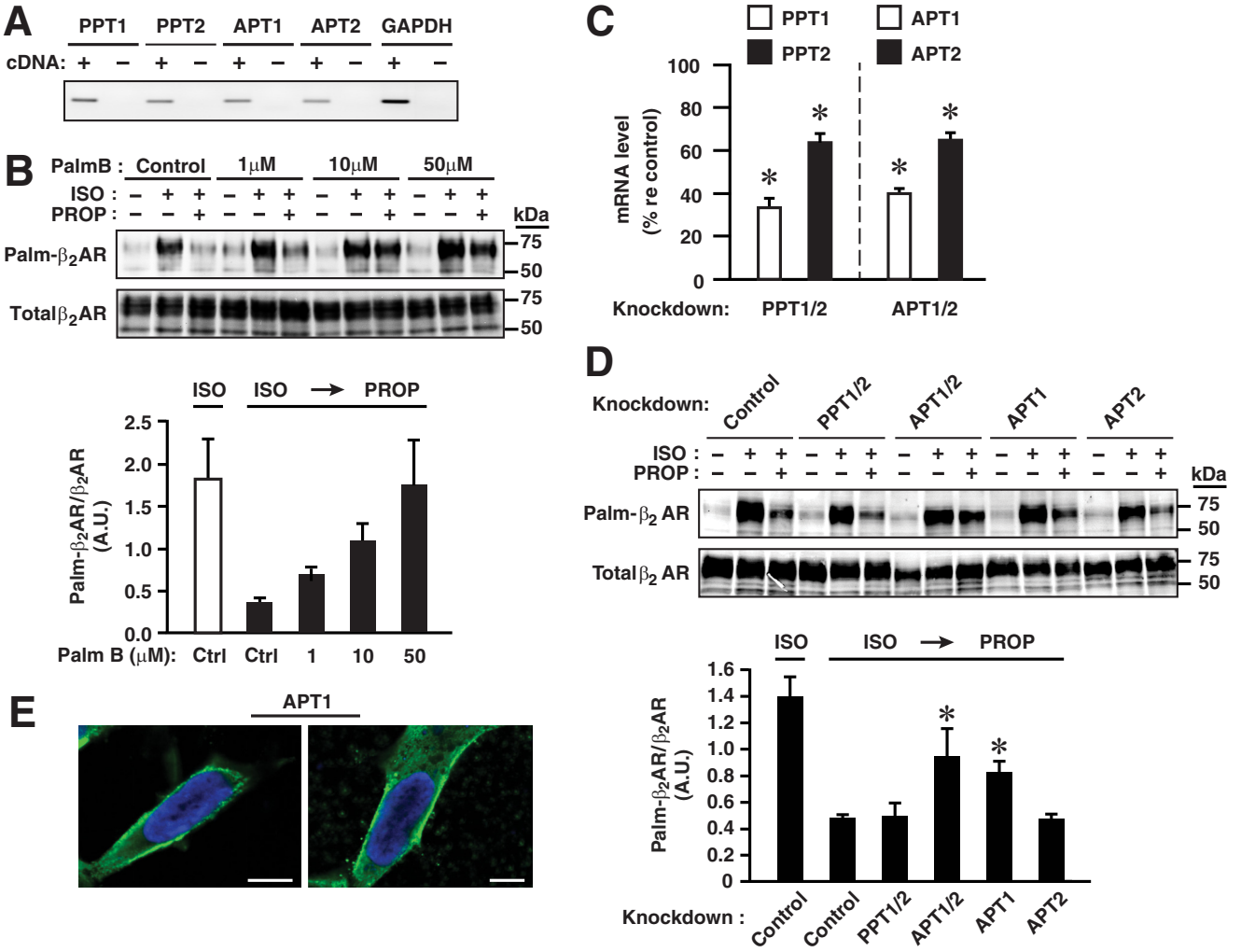

FIGURE 4. **β_2AR Cys-265 is depalmitoylated by APT1.** *A*, all four mammalian depalmitoylating enzymes (PPT1/2 and APT1/2) are expressed in HEK293 cells as assessed by qPCR. *B*, PalmB inhibits depalmitoylation of β_2AR-Cys-265 in a dose-dependent fashion after stimulation of *S*-palmitoylation with ISO (10 μM, 1 h) and truncation of stimulation with PROP (100 μM, 20 min) as revealed by acyl-RAC. $n = 4$. *A.U.*, arbitrary unit. *C*, knockdown of individual depalmitoylating enzymes with siRNA. $n = 3$; *, $p < 0.05$ *versus* control siRNA. *D*, knockdown with siRNA of depalmitoylating enzymes demonstrates that APT1 is responsible for depalmitoylation of β_2AR Cys-265. $n = 3$; *, $p < 0.05$ *versus* control siRNA plus ISO by ANOVA. *E*, confocal immunofluorescence microscopy shows that transfected (but untagged) APT1 (*green*) is localized principally to the plasma membrane. Hoechst 33342 was employed for nuclear staining (*blue*). *Scale bars* = 10 μm.

then phosphorylates Ser residues at two locations within the β_2AR: Ser-345/Ser-346 within the C-terminal tail and Ser-261/Ser-262 within the third intracellular loop (24). PKA-mediated phosphorylation has been associated with agonist-induced desensitization of the β_2AR (24) and with the regulation of coupling to G_i *versus* G_s (25), but distinct functions for PKA-mediated phosphorylation of Ser within the third intracellular loop *versus* the C-terminal tail remain poorly delineated. Ser-345/Ser-346 and Ser-261/Ser-262 are located adjacent to the canonical and newly discovered sites of *S*-palmitoylation, respectively. Because previous reports based on mutation of Cys-341 have suggested the possibility of cross-talk between *S*-palmitoylation of Cys-341 and phosphorylation of Cys-345/Cys-346 (26), we examined the possibility that agonist-induced *S*-palmitoylation of Cys-265 might be coupled functionally to phosphorylation of Ser-261/Ser-262.

Treatment of HEK293 cells stably expressing FLAG-tagged β_2AR-C341A with the PKA inhibitor H-89 (20 μM, 15 min) abrogated ISO-induced β_2AR *S*-palmitoylation (Fig. 6*A*). Inhibition by H-89 of ISO-induced Ser-262 phosphorylation was confirmed (Fig. 6*A*) by Western blotting with a monoclonal antibody specific for phospho-Ser-262 (27). Treatment with H-89 had no detectable effect on β_2AR internalization under these conditions (Fig. 6*B*). However, augmenting the cAMP levels by treatment of cells with the adenylyl cyclase activator forskolin, or the phosphodiesterase inhibitor 3-isobutyl-1-methylxanthine (IBMX), failed to induce *S*-palmitoylation, although the phosphorylation of Ser-262 was greatly enhanced (Fig. 6*C*). Therefore, PKA phosphorylation is necessary but not sufficient to induce receptor *S*-palmitoylation. Unlike stimulation by ISO, treatment with forskolin or IBMX did not induce receptor internalization (Fig. 6*D*). Thus, both PKA phosphorylation and internalization are required to induce receptor *S*-palmitoylation at Cys-265, consistent with the requirement that the receptor must traffic to the Golgi complex where zDHHC9/14/18 reside.

Treatment with H-89, which suppresses S-palmitoylation of Cys-265, would suppress ISO-induced PKA-mediated phos-

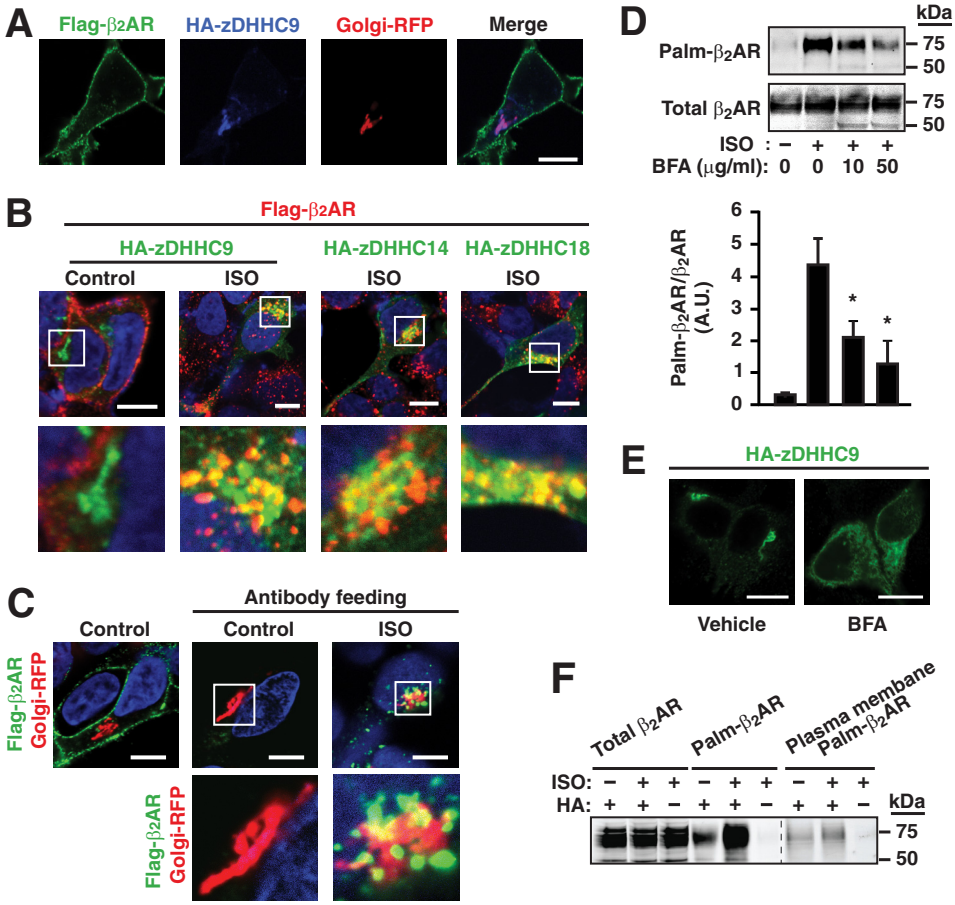

FIGURE 5. ***S*-Palmitoylation of β_2AR Cys-265 is associated with a previously undescribed intracellular itinerary.** *A*, confocal immunofluorescence microscopic analysis in HEK293 cells stably expressing FLAG-tagged wild-type β_2AR (*green*) and transiently transfected with HA-tagged zDHHC9 (*blue*) as well as the Golgi complex marker Golgi-RFP (*red*) under basal conditions. β_2AR is localized predominantly to the plasma membrane, whereas HA-zDHHC9 is localized to the Golgi complex. *B*, in HEK293 cells stably expressing FLAG-β_2AR (*red*), transiently transfected with HA-tagged zDHHC9, -14, or -18 (*green*), and stimulated with ISO (10 μM, 1 h), β_2AR are present at a perinuclear location (consistent with localization to the Golgi complex) where they co-localize with zDHHC9, -14, or -18. *Merged images* are shown at a relatively low and a higher magnification in the *top* (*white boxes*) and *bottom rows*, respectively. *Scale* bar = 10 μm. *C*, in HEK293 cells stably expressing FLAG-tagged wild-type β_2AR (*green*) and Golgi RFP, cell-surface FLAG-β_2AR was labeled with anti-FLAG M2 antibody in the absence or presence of 10 μM ISO for 30 min, and surface antibody was removed by acid wash. Hoechst 33342 was employed for nuclear staining (*blue*). This antibody feeding assay reveals directly that a population of β_2AR traffics from the plasma membrane to the Golgi complex upon ISO stimulation. *D*, treatment with brefeldin A (*BFA*) (50 μg/ml, 2 h) suppresses ISO-induced *S*-palmitoylation of β_2AR Cys-265 in a dose-dependent fashion. $n = 3$; *, $p < 0.05$ *versus* ISO without brefeldin A by ANOVA. *E*, treatment with brefeldin A (50 μg/ml, 2 h) results in delocalization of HA-zDHHC9 from a perinuclear concentration to a diffuse cytoplasmic distribution. *Scale bar* = 10 μm. *F*, cell-surface biotin labeling followed by acyl-RAC and then pulldown of biotinylated and *S*-palmitoylated proteins with streptavidin followed by Western blotting for the β_2AR demonstrates that at least some proportion of β_2AR *S*-palmitoylated at Cys-265 following ISO stimulation (10 μM, 1 h) returns to the plasma membrane following transit from the Golgi complex. Data shown are representative of two separate experiments.

phorylation of both Ser-261/Ser-262 and Ser-345/Ser-346 (28). To isolate the role of Ser-261/Ser-262, we examined the effect of mutation of Ser-261/Ser-262 to Ala-261/Ala-262 in β_2AR-C341A. Mutation of Ser-261/Ser-262 to Ala-261/Ala-262 greatly diminished ISO-induced *S*-palmitoylation (Fig. 6*E*). We considered two potential explanations for the obligate role of Ser-261/Ser-262 phosphorylation: phosphorylation might be required to route the β_2AR to the Golgi complex; and/or phosphorylation of Ser-261/Ser-262, closely adjacent to Cys-265, might exert an allosteric effect on *S*-palmitoylation *per se*. We could detect no effect of the S261A/S262A mutation on ISO-induced trafficking of the β_2AR to the Golgi complex as assessed by co-localization with DHHC9 (Fig. 6*F*) or by an antibody feeding assay (as in Fig. 5*C*), which directly demonstrated ISO-induced trafficking of plasma membrane-localized β_2AR bearing a S261A/S262A mutation to the Golgi complex, as shown by co-localization with Golgi-RFP (Fig. 6*G*). We therefore concluded that an allosteric mechanism is likely.

We also determined that activation of β_2AR-C341A by the endogenous β_2AR ligand epinephrine (10 μM, 2 h; parameters employed for all compounds tested) and by the synthetic β_2AR agonist fenoterol significantly enhanced *S*-palmitoylation of Cys-265, whereas exposure to norepinephrine or the synthetic agonist salbutamol or procaterol was much less efficacious (Fig. 7*A*). Although we found that, under these conditions, cAMP production was induced to a similar degree by these agonists (Fig. 7*B*), it has been shown that receptor internalization induced by stimulation with norepinephrine and salbutamol is substantially less efficacious *vis à vis* ISO or fenoterol (29, 30), which supports the dual determination of Cys-265 *S*-palmitoylation. In addition, exposure to any of a panel of 14 compounds classified as β_2AR antagonists or partial, inverse, or neutral ago-

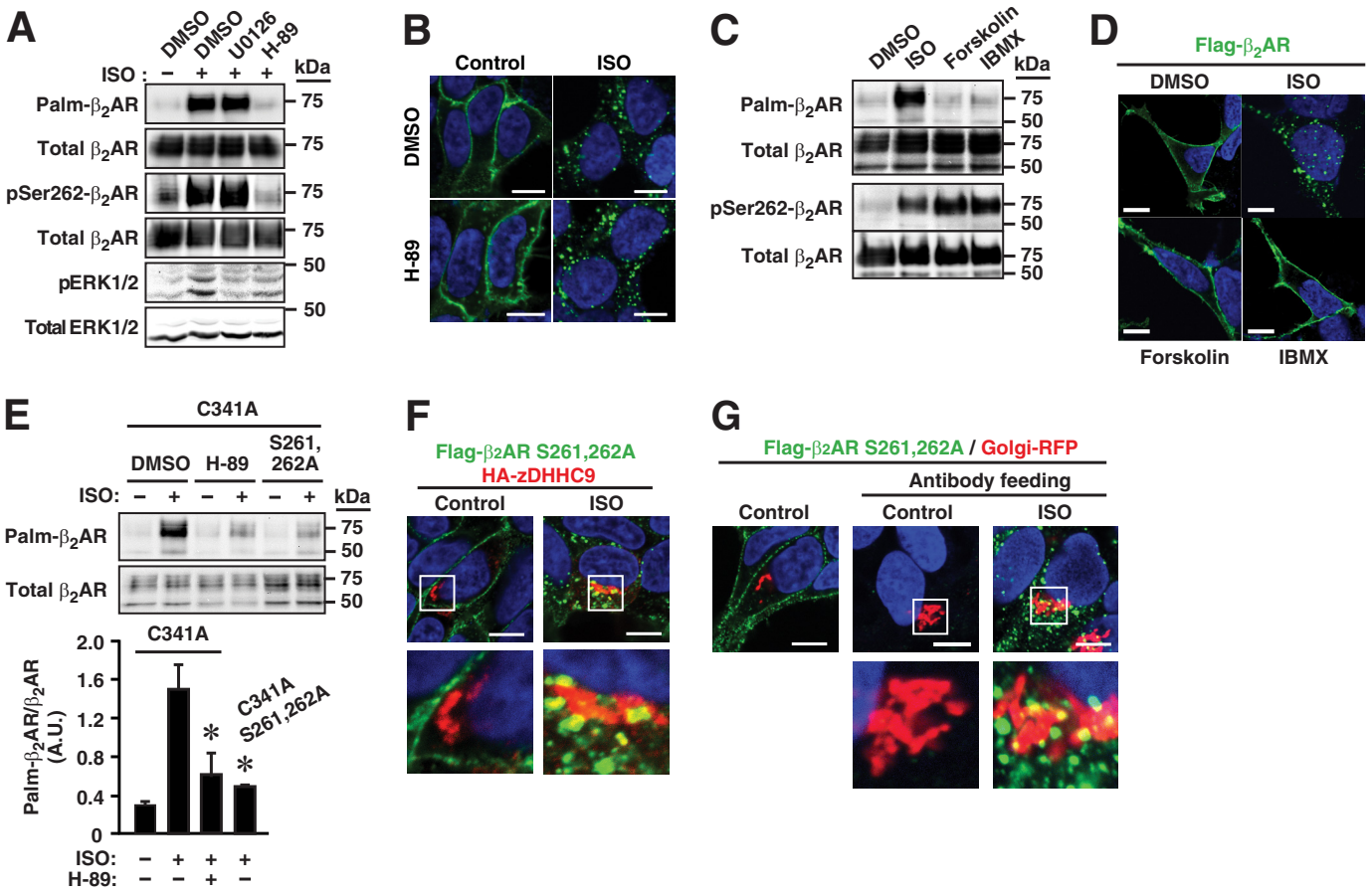

FIGURE 6. ***S*-Palmitoylation of β_2AR Cys-265 requires PKA-mediated phosphorylation of Ser-261/Ser-262.** *A*, in W9 cells, ISO-induced *S*-palmitoylation of Cys-265 is eliminated by inhibition of PKA with H-89 (20 μM, 15-min pretreatment), which eliminates phosphorylation of Ser-262, whereas treatment with U0126 (100 μM, 15 min pretreatment) to inhibit MAPK-dependent signaling, as verified by suppressed phosphorylation of ERK, had no effect on *S*-palmitoylation of Cys-265. *B*, in W9 cells, treatment with H-89 (20 μM, 15 min prior to ISO) had no detectable effect on ISO-induced (10 μM, 1 h) internalization of β_2AR. *C*, neither the adenylate cyclase activator forskolin (50 μM, 1 h) nor the phosphodiesterase inhibitor IBMX (200 μM, 1 h) induced *S*-palmitoylation of Cys-265, although phosphorylation of Ser-262 was greatly enhanced. *D*, unlike ISO (10 μM, 1 h), neither forskolin nor IBMX induced β_2AR internalization. *E*, mutation of Ser-261/Ser-262 greatly attenuates ISO-induced *S*-palmitoylation. DMSO = vehicle control. $n = 3$; *, $p < 0.05$ *versus* ISO C341A by ANOVA. *F*, mutation of Ser-261/Ser-262 has no apparent effect on ISO-induced co-localization of FLAG-tagged- β_2AR (*green*) with HA-zDHHC9 (*red*). In *F* and *G*, *merged images* are shown at a relatively low (*white boxes*) and a higher magnification in the *top* and *bottom rows*, respectively. Hoechst 33342 was employed for nuclear staining (*blue*). *Scale bars* = 10 μm. *G*, labeling of FLAG-tagged β_2AR with anti-FLAG Ab prior to ISO stimulation directly demonstrates trafficking of plasma membrane-localized β_2AR to the Golgi complex, identified by Golgi-RFP (antibody feeding assay).

nists had no effect (Fig. 7*C*); this includes carvedilol, a formal antagonist that has been shown to activate β-arrestin-mediated signaling (31). Ligand-induced signaling via β-arrestins involves activation of MAPK-dependent transduction (32). Consistent with the failure of carvedilol to induce Cys-265 palmitoylation, treatment with the MEK/ERK inhibitor U0126 had no effect on ISO-induced Cys-265 palmitoylation (Fig. 6*A*), although ERK phosphorylation was suppressed (Fig. 6*A*). Thus, Golgi complex-directed trafficking and Cys-265 *S*-palmitoylation of β_2AR are apparently uninfluenced by β-arrestin-mediated signaling.

Altered Membrane Stability and Signaling Consequent upon S-Palmitoylation of Cys-265 within β_2AR—Our results indicate that a population of β_2AR undergoes a tightly regulated, dynamic cycle of *S*-palmitoylation/depalmitoylation that entails traffic to the Golgi complex (zDHHC9/14/18) and a return to the plasma membrane (APT1). We used PalmB in combination with ISO stimulation to enhance the population of plasma membrane-localized, Cys-265 *S*-palmitoylated β_2AR to elucidate the effects of Cys-265 *S*-palmitoylation on β_2AR disposition and ligand-induced signaling.

We first examined trafficking of the wild type *versus* β_2AR-C265A induced by stimulation with ISO followed by truncation of stimulation by PROP in the presence or absence of PalmB. As assessed by fluorescence-activated cell sorting, the steady-state proportion of receptors internalized as a result of ISO-stimulation (10 μM, 60 min) did not differ significantly in cells expressing the wild type or β_2AR-C265A and also was unaffected by PalmB (Fig. 8*A*, 0 min). The time course of re-establishment of plasma membrane-localized receptors during PROP treatment also did not differ (Fig. 8*A*). However, the abundance of plasma membrane-localized wild-type receptors following truncation of ISO stimulation was substantially (~50%) enhanced by treatment with PalmB, an effect that was eliminated by mutation of Cys-265 (Fig. 8*A*). Because the abundance of the plasma membrane-localized receptor under these conditions will reflect competing mechanisms of membrane addition and removal of the receptor following the addition of PROP (including ligand-independent (basal) turnover (33)), this result indicates that β_2AR is stabilized at the plasma membrane by *S*-palmitoylation of Cys-265.

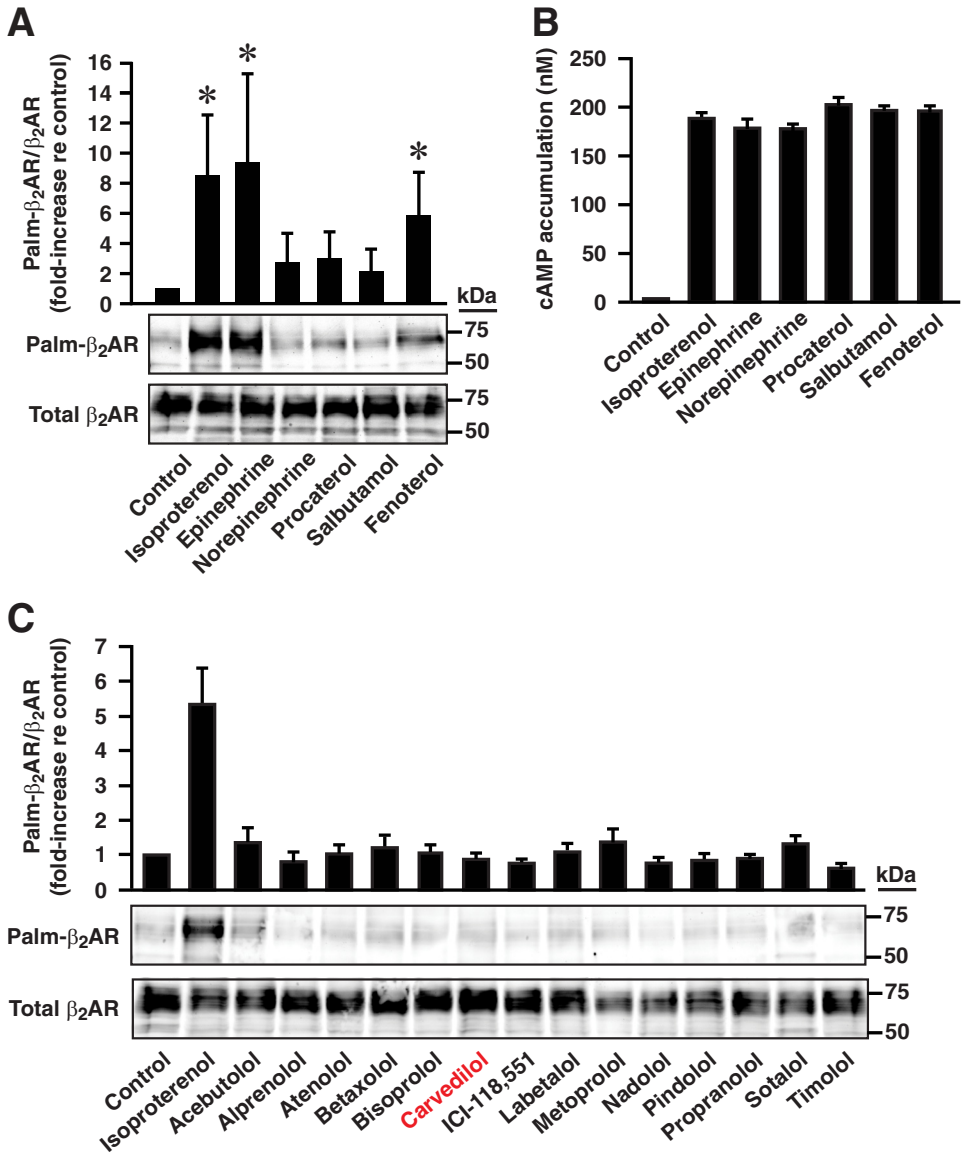

FIGURE 7. ***S*-Palmitoylation of Cys-265 and cAMP production induced by stimulation with a battery of pharmacological agents.** *A*, *S*-palmitoylation of Cys-265 was enhanced by the endogenous β_2AR ligand epinephrine and the synthetic agonist fenoterol but not by norepinephrine, procaterol, or salbutamol (10 μM, 2 h). $n = 6$; *, $p < 0.05$ *versus* unstimulated control by ANOVA. *B*, all agents employed in *A* (10 μM, 5 min) enhanced cAMP production to a similar extent. *C*, none of a battery of 14 additional agents acting on the β_2AR enhanced the *S*-palmitoylation of Cys-265, including carvedilol, which signals through β-arrestins (10 μM, 2 h).

To investigate the possible changes in signaling through β_2AR *S*-palmitoylated at Cys-265 that would support the ascription of a distinct trafficking itinerary, we employed stimulation with ISO (1 μM, 1 h) in combination with PalmB treatment (50 μM) to maintain the population of plasma membrane-localized β_2AR *S*-palmitoylated at Cys-265 followed by truncation of ISO-induced activation by treatment with PROP (1 μM, 1 h) in the presence of PalmB and restimulation with ISO (10 μM, 5 min). We first verified that Cys-265-*S*-palmitoylated and plasma membrane-localized β_2AR were preserved in the presence of PalmB during PROP treatment following the initial ISO stimulation (Fig. 8*B*), employing cell-surface biotin labeling followed by acyl-RAC, pull-down of biotinylated proteins with streptavidin, and Western blotting for the β_2AR (as in Fig. 5*D*). Ligand-induced activation of β_2AR elicits signaling via G protein (resulting in altered production of cAMP via $G_{s/i}$) and activation of MAPK-based transduction via both G_i and β-arrestin (34). We found that after cAMP returned to basal levels during exposure to PROP, cAMP production induced by restimulation with ISO (10 μM, 5min) of wild-type β_2AR was significantly suppressed in the presence of PalmB (Fig. 8*C*). Suppression of ISO-induced cAMP production by PalmB was eliminated by mutation of Cys-265 (Fig. 8*C*). MAPK-based signaling as assessed by ERK phosphorylation was also modestly suppressed by treatment with PalmB, dependent upon Cys-265 (Fig. 8, *D* and *E*). Inhibition of both cAMP production and ERK phosphorylation by *S*-palmitoylation of Cys-265 is consistent with a direct effect on ligand-induced activation. However, we do not exclude alternative explanations for diminished activity including the effects of *S*-palmitoylation on the subcellular disposition of the receptor that

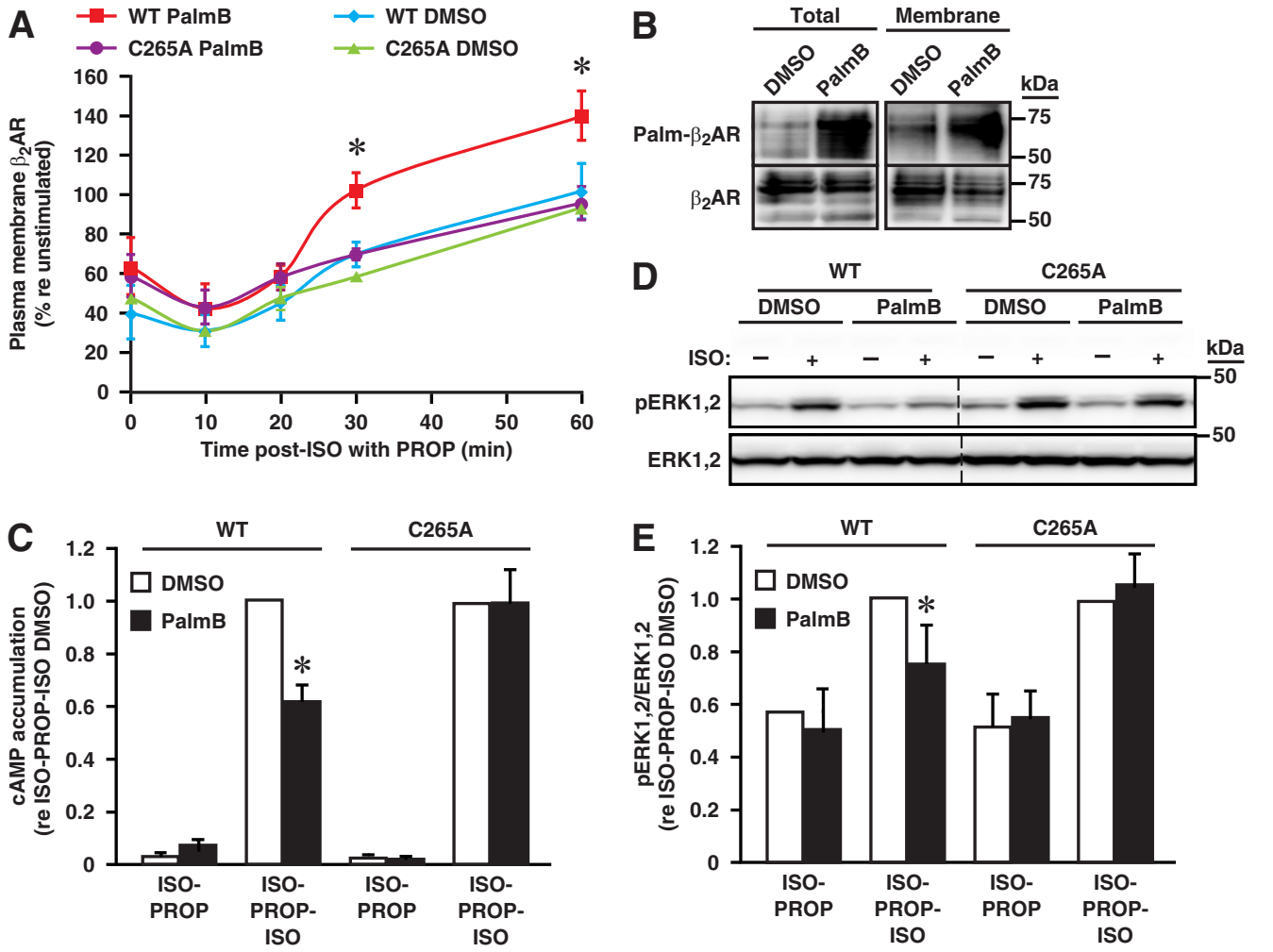

FIGURE 8. **Disposition of and transduction through β_2AR *S*-palmitoylated at Cys-265.** *A*, following ISO-induced (10 μM, 1 h) β_2AR internalization (40–60% internalization at time 0), exposure to PROP (100 μM) is accompanied by increasing plasma membrane abundance of WT and β_2AR-C265A along a similar time course in the presence or absence of PalmB (50 μM) as assessed by FACS. However, the plasma membrane abundance of wild-type β_2AR but not β_2AR-C265A is significantly enhanced by PalmB. $n = 3$; *, $p < 0.05$. *B*, cell-surface biotin labeling followed by acyl-RAC and pulldown of biotinylated and *S*-palmitoylated proteins with streptavidin followed by Western blotting for β_2AR demonstrates that *S*-palmitoylated Cys-265 and plasma membrane-localized β_2AR are preserved by PalmB following ISO stimulation (1 μM, 1 h) and exposure to PROP (1 μM, 1 h) Results shown are representative of three separate experiments. *C*, following stimulation with ISO (1 μM, 1 h) followed by suppression of stimulation with PROP (1 μM, 1 h) in the presence of PalmB to maintain *S*-palmitoylation, restimulation with ISO (10 μM, 5 min) results in cAMP production that is significantly suppressed by *S*-palmitoylation of Cys-265 within the β_2AR. $n = 6$; *, $p < 0.01$ by ANOVA. *D*, following stimulation with ISO followed by PROP in the presence of PalmB to maintain *S*-palmitoylation, restimulation with ISO results in ERK phosphorylation that is suppressed by *S*-palmitoylation of Cys-265 within β_2AR. See *E* for quantification. $n = 6$; *, $p < 0.01$ by ANOVA.

result in diminished access to ligand or altered $G_{s/i}$ coupling. Note that the suppression of signaling under these conditions is evident, despite the fact that the abundance of plasma membrane-localized β_2AR is enhanced in the presence of PalmB (Fig. 8*A*).

Discussion

We report here that a population of β_2AR, a canonical heptahelical transmembrane receptor, embarks on a previously unreported intracellular itinerary following ligand-induced activation that is associated with phosphorylation of Ser-261/Ser-262 within the third intracellular loop, and that takes them to the Golgi complex, where they are *S*-palmitoylated at Cys-265 within the third intracellular loop by zDHHC9/14/18 (a distinct subfamily of the zDHHC family of palmitoyl transferases), and from whence they traffic to the plasma membrane, where they are depalmitoylated by APT1. To our knowledge, trafficking from the plasma membrane to the Golgi complex has not been reported for any βAR.

Dynamic S-Palmitoylation of β_2AR—Earlier demonstrations of the ligand-induced dynamic turnover of palmitate on β_2AR were interpreted on the assumption that Cys-341 was the sole site of *S*-palmitoylation (4), but turnover of palmitate on β_2AR lacking Cys-341 has not been examined previously. Our results demonstrate that the ligand-induced dynamic turnover of palmitate on β_2AR reflects predominantly *S*-palmitoylation/depalmitoylatiom of the previously unreported site of *S*-palmitoylation, Cys-265. In this regard, it is of note that, as reported recently, β_1AR is *S*-palmitoylated at Cys-392/Cys-393, equivalent to Cys-341 within β_2AR, and also at a more distal site within the C-terminal tail, Cys-414, and that (basal) turnover at the distal site is much greater than at the proximal site (35); that is, *S*-palmitoylation of the canonical GPCR consensus Cys within β_1AR is relatively stable, as we have shown for β_2AR.

Determinants of Cys-265 S-Palmitoylaytion—*S*-Palmitoylation of Cys-265 is predominantly dependent upon ligand-induced activation of β_2AR and both the consequent phosphorylation of Ser-261/Ser-262 and receptor internalization. Because mutation of Ser-261/Ser-262 does not detectably affect ligand-induced trafficking of β_2AR to the Golgi complex, the effect of the phosphorylation of Ser-261/Ser-262 on the *S*-palmitoylation of Cys-265 is likely allosteric. This is the first example of which we are aware of allosteric regulation of zDHHC-mediated *S*-palmitoylation. Although most previous analyses describe the regulation of β_2AR function by phosphorylation of Ser-261/Ser-262 and Ser-345/Ser-346 in combination (24, 25), we have demonstrated a role for Ser-261/Ser-262 phosphorylation specifically: the regulation of Cys-265 palmitoylation. It is of interest that *S*-palmitoylation of H-Ras (the first mammalian protein shown to be endogenously *S*-palmitoylated) targets Cys-181/Cys-184 (36), mediated at least in part by zDHHC9 (21), and that Ser-183 is reportedly a site of phosphorylation within H-Ras (37).

Enzymatic Regulation of Cys-265 S-Palmitoylation and Receptor Subtype Specificity—Enzymatic regulation of *S*-palmitoylation/depalmitoylation in mammals is mediated respectively by the 23 members of the zDHHC family and the four depalmitoylating enzymes, PPT1/2 and APT1/2. Elucidation of the substrate specificities of the zDHHC family and PPT/APT enzymes remains incomplete. Our results demonstrate that *S*-palmitoylation of Cys-265 is mediated by zDHHC9/14/18, which constitute a distinct subfamily of the 23 mammalian zDHHC, and that depalmitoylation is mediated selectively by APT1. Thus, our results indicate marked specificity of the enzymatic mechanisms of *S*-palmitoylation/depalmitoylation that operate under physiological conditions.

Both β_2AR and β_1AR are *S*-palmitoylated at a canonical site within the C-terminal tail, but only β_2AR is *S*-palmitoylated at Cys-265 within the third intracellular loop. Functional differences between β_2AR and β_1AR are well known (38, 39) and include the fact that, in contrast to β_1AR, β_2AR are preferentially localized under basal conditions to caveolae and/or lipid rafts from which they transit upon agonist-induced stimulation (39). It is also well known that *S*-palmitoylation is associated with the localization of modified substrates to caveolae and/or membrane rafts (40). Structural analysis indicates that Cys-265 resides in a juxtamembrane position (33), consistent with plasma membrane anchoring in caveolae/lipid rafts by *S*-palmitoylation of Cys-265. Thus, perhaps differential coupling by β_2AR *versus* β_1AR to G_i (38) (also preferentially localized to caveolae/lipid rafts by virtue of *S*-palmitoylation of $G_i\alpha$ (41)) may be facilitated by *S*-palmitoylation of Cys-265 within β_2AR under potential conditions in which *S*-palmitoylation of Cys-265 is sustained.

Effect on Signal Transduction of S-Palmitoylation of Cys-265—It should be emphasized that our experimental conditions (Fig. 8, PalmB effects on cAMP production and ERK phosphorylation following stimulation with ISO, truncation of stimulation with PROP, and restimulation with ISO), which revealed the suppression of transduction by S-palmitoylation, were not designed to assess the effects of *S*-palmitoylation on physiological signaling *per se* but rather to examine changes in second messengers and downstream effectors as evidence for trafficking to the plasma membrane of a unique micropopulation of receptors that is increasingly represented at the cell surface during sustained stimulation. Indeed, it is quite conceivable that the principal role of the *S*-palmitoylation of Cys-265 is to regulate signaling at the Golgi complex (see below), which remains to be tested in future experiments. With that said, our results indicate that inhibition of the depalmitoylation of Cys-265 within the β_2AR is associated with diminished ligand-induced signaling by both G protein and β-arrestin under our experimental conditions. This suppression might result from a direct effect of *S*-palmitoylation on receptor activation and/or altered membrane compartmentalization of the β_2AR, which alters accessibility to ligand and/or coupling to downstream effectors. However, other components of the β_2AR signalsome are modified by *S*-palmitoylation, including G protein α-subunits (41, 42), and our results do not rule out the effects of PalmB on the depalmitoylation of relevant elements other than β_2AR itself. It is of note that Cys-265 is closely adjacent to Glu-268 at the cytoplasmic end of transmembrane domain VI, which provides one side of the "ionic lock" that constrains β_2AR (43). Consequent conformational change upon release from the ionic lock is thought to be a key step in receptor activation (43, 44). Stabilization of the conformation maintained by the ionic lock by *S*-palmitoylation of Cys-265, perhaps due to membrane anchoring, would be consistent with inhibition of signaling by both G protein and β-arrestin. Thus, our findings suggest that depalmitoylation at the plasma membrane may sustain the ligand-induced trafficking cycle.

S-Palmitoylation of Cys-265 in Cellular Context—In vivo, β_2AR are subject to basal stimulation, modulated up and down with "sympathetic tone." Our findings suggest that, under pathophysiological conditions of heightened and sustained adrenergic stimulation that result in β_2AR desensitization and down-regulation, the relative abundance of β_2AR that are *S*-palmitoylated at Cys-265 will be greatly enhanced. It is well established that down-regulation of β_1AR, and to a lesser extent β_2AR, results from heightened and sustained adrenergic stimulation that is a concomitant of heart failure (45) and other conditions including severe burns (46), representing a principal homeostatic mechanism to counterpose adrenergic drive. Our findings indicate that enhancement of the relative abundance of the population of β_2AR *S*-palmitoylated at Cys-265 during sustained stimulation represents a signature of selective preservation of β_2AR.

Finally, our finding that a population of β_2AR follows a novel intracellular itinerary via the Golgi complex that entails *S*-palmitoylation of Cys-265 (distinct from the well characterized routes of endosomal recycling to the plasma membrane or routing into degradative pathways) suggests that Golgi complex-localized β_2AR may play a distinct functional role. It has recently been shown that internalized β_2AR mediate intracellular signal transduction from an endosomal compartment (47), and our results are consistent with the proposition that Golgi complex-localized β_2AR represent a distinct intracellular signaling platform (operative selectively for β_2AR *versus* β_1AR) regulated by *S*-palmitoylation of Cys-265. In this regard, it is of note that at least one prominent

component of the β_2AR signalsome, endothelial nitric-oxide synthase, is localized to and active at both the plasma membrane and Golgi complex (48).

Experimental Procedures

Reagents and Plasmids—All materials were from Sigma-Aldrich unless otherwise specified. PalmB was from EMD-Millipore, and thiopropyl-Sepharose was from GE Healthcare. Sources of primary antibodies were as follows: rabbit anti-β_2AR antibody (sc-569) was from Santa Cruz Biotechnology; mouse anti-HA antibody (catalogue No. 2367) from Cell Signaling; and rabbit anti-ERK2 antibody (sc-154) from Santa Cruz Biotechnology. Anti-β_2AR pS262 antibody (clone 2G3) was kindly provided by Dr. Richard B. Clark. Alexa Fluor 488- and 594-conjugated secondary antibodies were from Invitrogen. Horseradish peroxidase-conjugated secondary antibodies were from Jackson ImmunoResearch. IRDye-conjugated secondary antibodies were from LI-COR Biosciences. pEF-Bos-HA-ZDHHC plasmids were kindly provided by Dr. Masaki Fukata. Mutations converting cysteine to alanine and serine to alanine were individually introduced into FLAG-human β_2AR/pcDNA3 by site-directed mutagenesis. All resulting plasmids were verified by DNA sequencing.

Reverse Transcription and Real-time PCR—RNA was extracted using TRIzol RNA isolation reagents (Invitrogen), and 3 μg of RNA was used to prepare cDNA with random hexamer oligonucleotide primers using the SuperScript III first-strand synthesis system for RT-PCR (Invitrogen). Gene-specific primers were used for real-time PCR in a StepOnePlus real-time PCR system (Applied Biosystems) using iTaq SYBR Green Supermix with ROX (Bio-Rad). The expression of GAPDH in each sample was used to normalize the expression of the genes of interest. Real-time PCR primers are listed in Table 1. The -fold change in expression was calculated using the comparative C_t method.

Cell Culture and Transfection and siRNA-mediated Knockdown—HEK293 cells were maintained in minimum essential media with 10% fetal bovine serum, 100 units/ml penicillin, and 100 μg/ml streptomycin at 37 °C in a humidified 5% CO_2 atmosphere. Cells were transfected at ~70% confluence using Lipofectamine LTX (Invitrogen) according to the manufacturer's instructions. To generate stable cell transfectants, G418 (Invitrogen) was added to a final concentration of 150 μg/ml of active antibiotic. HEK cell lines stably overexpressing FLAG-β_2AR were kindly provided by Dr. Robert Lefkowitz. Predesigned siRNA, siGENOME SMARTpool for ZDHHC and ON-TARGETplus SMARTpool for PPTs and APTs were obtained from Thermo Scientific. siRNA were transfected at ~30% confluence using Lipofectamine RNAiMAX (Invitrogen) according to the manufacturer's reverse transfection protocol. Cells were assayed ~72 h later. To visualize the Golgi complex, CellLight Golgi-RFP, BacMam 2.0 (Molecular Probes) was used according to the manufacturer's protocol.

FACS and Cell-surface Biotinylation—Flow cytometry was performed essentially as described previously (49). After 2 h of serum starvation, HEK cells stably overexpressing wild-type or C265A FLAG-β_2AR were stimulated with ISO (10 μM; 1 h) and then treated with PROP (100 μM) for specified intervals in the presence or absence of PalmB (50 μM). Cells were then washed with PBS and harvested by trypsinization. The collected cells were incubated with anti-DDDDK tag mAb Alexa Fluor 488 (2.5 ng/μl) (MBL International Corp., M185-A48) for 30 min on ice. After washing, cells were fixed with 1% paraformaldehyde for 15 min and then analyzed with a FACSAria III (BD Biosciences). Cells incubated with Alexa Fluor 488-labeled mouse IgG2a (MBL International Corp., M076-A48) served as controls.

For cell-surface biotinylation of *S*-palmitoylated β_2AR, cells were treated as described for FACS but with a 1-h exposure to ISO followed by a 1-h exposure to PROP in the presence or absence of PalmB. Then they were incubated with EZ-Link Sulfo-NHS-LC-biotin (Thermo Fisher Scientific) (0.5 mM, 30 min at 4 °C). After washing, the biotin-labeled cells were subjected to acyl-RAC. *S*-Palmitoylated proteins were eluted from the thiopropyl-Sepharose beads with 0.25% β-mercaptoethanol, and unreacted β-mercaptoethanol was rendered inactive (quenched) with an excess of L-cystine prior to isolation of biotinylated and *S*-palmitoylated proteins with streptavidin-agarose beads, which were eluted by boiling with SDS sample buffer. Western blotting was done with an anti-β_2AR antibody (SC-569, Santa Cruz Biotechnology).

Assay of cAMP and Phospho-ERK—HEK cell lines stably overexpressing wild-type or Cys265Ala FLAG-β_2AR were stimulated with ISO (1 μM, 1 h) followed by treatment with PROP (1 μM, 1 h) in the presence or absence of PalmB (50 μM). Cells were then restimulated with ISO (10 μM; 5 min). For the assay of cAMP, restimulation with ISO was carried out in the presence of the phosphodiesterase inhibitor 4-(3-butoxy-4-methoxybenzyl) imidazolidin-2-one (20 μM, Sigma-Aldrich). The washed cells were then collected, and cAMP was assayed with a cAMP Parameter Assay kit (R&D Systems) according to the manufacturer's instructions. After identical treatment, phospho-ERK was assayed as described previously (34). Phospho-p44/42 MAPK (ERK1/2) (Thr-202/Tyr-204) antibody (9101S, Cell Signaling) and ERK2 (C-14) antibody (sc-154, Santa Cruz Biotechnology) were used to detect phospho-ERK1/2 and total ERK1/2, respectively.

Detection of S-Palmitoylation by acyl-RAC—The acyl-RAC method was applied essentially as described (6, 7) with minor modifications. Cells in a 6-well plate were harvested and lysed in 100 μl of lysis buffer (50 mM Tris-HCl, 150 mM NaCl, 5 mM EDTA, 1% Nonidet P-40, and 10% glycerol, pH 7.4) containing protease inhibitor mixture (Roche). After trituration by repeated pipetting, lysates were centrifuged at 20,000 × *g* for 15 min at 4 °C. The supernatants were then diluted in 300 μl of blocking buffer (100 mM HEPES, 1 mM EDTA, 2.5% SDS, and 0.1% methyl methanethiosulfonate, pH 7.4) and incubated at 50 °C for 10 min. Following acetone precipitation twice, the pellets were washed with 70% acetone and resuspended in binding buffer (100 mM HEPES, 1 mM EDTA, and 1% SDS, pH 7.4). Total protein was quantified with a bicinchoninic acid (BCA) assay (Pierce) using BSA as the standard, and equal amounts of protein (50–200 μg) were rediluted in 150 μl of binding buffer. Approximately 50 μg of protein from each sample was retained to assess input. When employed, an equal volume of freshly prepared 1 M NH_2OH, pH 7.2, was added followed by ~30 μl of prewashed thiopropyl-Sepharose. Binding was carried out on a rota-

TABLE 1
Real-time PCR primers employed

Real-time PCR Primers for zDHHCs

ZDHHC	AC No.	Forward Primer	Reverse Primer
1	NM_013304	CCTATGAGTACATCGTGCAGC	ATATGTCTGAAGGTCCGCATG
2	NM_016353	CATCAGGAAGTTCTTAGGCGAG	ACATTTATCACAGACGGAGCAG
3	NM_001135179	ACAACTGTGTAGGCGAGAAC	AGAGAAGGAGCTGCACTTTG
4	NM_001134388	TGTTCTTATCTGCGTCTGCTC	AAGGTGTGGTTTCTCGTATGG
5	NM_015457	CTAAGCCTGTATGTGTCACCTGTCTTCACAA	CATCTTCCTTGTCCTCATCCTC
6	NM_022494	GTCCCTGCAC	CCAACCCCTTATTCTTGAAACAC
7	NM_017740	CTTCTGGTACTCTGTGGTCAAC	CTTTCGTAGCGTTTCCTTTGG
8	NM_013373	ACGCTGGTTAAGAAGGTGTC	GGGCAGAGAAGTTGGTGG
9	NM_016032	ATGGCTACACTGTTGAGGAC	ATTCTTGATACGAGGCGGTG
11	NM_024786	GCAAATGGACAAAGGAGTTCTC	CCCCATCCTGGTTTACTGAAG
12	NM_032799	ACTTCTTCTGTGGATGGCC	TTTCAGGCACAAGACGGTAG
13	NM_019028	TGTAAATGGGCAGACACCTC	GTGAAGTGGAGTGTTTTGGTG
14	NM_024630	CGTTCACAGCAAACAGGATTC	GGTTGGAGCTGATCAAGTAGG
15	NM_144969	TGCTCGTTATTGTCCTCGTC	CTTCCAGTAGGTCCAGGTAAAG
16	NM_032327	AAGGGCAGAGTATTTAGGAATCC	GGGCAAGTGACTAGAAGGTAAG
17	NM_015336	TGAATGCCAGGAGATACAAGC	CACGATAACAGGACGAAAGAGG
18	NM_032283	CATCGCTGCCATCCTCTTC	CGGTATGTAGAACTGCCTGTG
19	NM_001039617	GTCACCTGTCTCATCTTCCTG	GACAGTGCCTGGATCAGC
20	NM_153251	TCAGCCTGTGACTCATGTATTC	CTGTTGCAGCCACGAAAAG
21	NM_178566	CTGTCTGGTTGCCTTAGTGAG	AGTGATGGGAACGCTTTGG
22	NM_174976	TCAATGTCGGAAGTGAGAGC	GGTTGTAGTGAGTCATGGGTG
23	NM_173570	CGGATATGTGGCATCTGTGT	GTGTCCAAGGTCAGTGTGATC
24	NM_207340	GATCACCTTCCAGACCACAG	CCAACCCGACTTCCTTACTG

Real-time PCR primers for PPTs, APTs and GAPDH

Protein	AC No.	Forward Primer	Reverse Primer
PPT1	NM_001142604	TCGCAACCACAGCATCTTC	CCAAACCACTCCGAATCTACAG
PPT2	NM_005155	GTCTAACCTCTATCGGATCTGC	GGTCTCTTTCCCCATTGATCAG
APT1	NM_006330	GCAATAACATGTCAACCCCG	GTGAACTTCTGATACCTGCAAAG
APT2	NM_007260	GGCAGCTGTGAAGGAATTTC	CCGGCTCAGATCCAAGATG
GAPDH	NM_001256799	ACATCGCTCAGACACCATG	TGTAGTTGAGGTCAATGAAGGG

tor at room temperature for 2 h. The resin was washed four times with binding buffer and eluted in 30 μl of SDS sample buffer containing 1% 2-mercaptoethanol at 42 °C for 10 min prior to SDS-PAGE and Western blotting.

Detection of S-Palmitoylation by Metabolic Labeling and Click Chemistry—Metabolic labeling and click chemistry were carried out essentially as described (10) with minor modifications. HEK293 cells stably expressing wild-type or Cys265Ala

FLAG-β_2AR were cultured in 100-mm dishes and incubated with 30 μM 17-octadecynoic acid (Cayman Chemical) and 5 μg/ml cerulenin in labeling medium (minimum Eagle's medium containing 5% dialyzed FCS (Gemini BioProduct)) for 1 h followed by stimulation with 10 μM ISO for 1 h. The cells were then washed and solubilized by sonication in ice-cold PBS containing 50 μM PalmB and protease inhibitor mixture. To concentrate the membrane fraction, cell lysates were centrifuged at 100,000 $\times$ *g* for 45 min at 4 °C. The pellets were resuspended in lysis buffer and subjected to methanol-chloroform precipitation to remove excess probe and other probe-incorporated metabolites. The pellets were then resuspended in 1.2% SDS in PBS. After measuring the protein concentration, lysate containing 300 μg of total protein was adjusted to a reaction volume of 300 μl containing 100 μM azide-PEG3-biotin (Sigma), 1 μM neutralized tris(2-carboxyethyl)phosphine (TCEP), 100 μM tris[(1-benzyl-1*H*-1,2,3-triazol-4-yl)methyl]amine dissolved in DMSO/*tert*-butanol (20:80%), and 1 μM $CuSO_4$ (final reagent volume adjusted with PBS) and incubated for 1 h at room temperature in the dark. The proteins were then precipitated with chloroform-methanol, and the resultant pellets were dissolved in 120 μl of 1% SDS in PBS. 20 μl of solubilized proteins was retained to assess total input, and the remaining 100 μl was incubated with 30 μl of streptavidin-agarose in 1 ml of lysis buffer for 1 h at room temperature. After washing, the samples serving as specificity controls were incubated with 1 M hydroxylamine, pH 7.4, for 1 h at room temperature. The biotinylated proteins were eluted with 30 mM D-biotin in 2% SDS at 42 °C. For Western blotting analysis, the eluted proteins were resolved by SDS-PAGE and visualized with anti-β_2AR antibody. Western blotting signals were analyzed as done for acyl-RAC. The values obtained for *S*-palmitoylated β_2AR were normalized with respect to total β_2AR.

Detection of Phosphorylation of β_2AR Ser-262—HEK293 cells stably expressing FLAG-β_2AR-C341A were harvested and lysed in 300 μl of lysis buffer containing protease inhibitor mixture and PhosSTOP phosphatase inhibitor mixture (Roche Applied Science). FLAG-β_2AR-C341A was immunoprecipitated using anti-FLAG M2 affinity gel for 30 min at 4 °C and washed three times with lysis buffer. FLAG-β_2AR-C341A was eluted in 30 μl of SDS sample buffer containing 1% 2-mercaptoethanol at 42 °C for 10 min followed by Western blotting. Phosphorylation of Ser-262 was visualized specifically with an anti-pS262 antibody (47, 48).

Immunofluorescence Staining and Confocal Imaging—Cells in glass-bottom dishes were fixed with 4% paraformaldehyde/PBS, permeabilized with 0.1% Tween 20 in PBS for 10 min, and incubated in 10% normal goat serum/PBS containing 0.1% Tween 20 for 30 min. After blocking, the cells were incubated with the appropriate primary antibody for 2 h at room temperature or overnight at 4 °C followed by the respective fluorescence-tagged secondary antibody. Immunostaining was assessed by confocal immunofluorescence microscopy (Carl Zeiss, LSM700).

Antibody Feeding Assay—Antibody feeding assays were performed essentially as described (35). Briefly, cells were fed 1 μg/ml anti-FLAG M2 antibody in the presence or absence of 10 μM ISO at 37 °C for 30 min. After washing with PBS, cell-surface antibody was removed by an acid wash (0.5 M NaCl and 0.5% acetic acid, pH 1.0) for 1 min. To visualize internalized antibody, cells were washed with PBS, fixed, permeabilized with 0.1% Tween-20, and incubated with the respective fluorescence-tagged secondary antibody.

Western Blotting Analysis, Data Presentation, and Statistics—Western blotting signals were detected using the ChemiDoc XRS system (Bio-Rad) or ODYSSEY® CLx (LI-COR Biosciences), and densitometric analysis was performed with Quantity One or Image Studio software, respectively. All comparisons were made between bands on a single blot. Densitometric values for *S*-palmitoylated β_2AR were normalized with respect to total β_2AR or in the analysis of cellular abundance of *S*-palmitoylated β_2AR (Fig. 1*E*) with respect to tubulin (which was unaffected by treatment).

All Western blotting data shown are from single blots at a single exposure. Within-blot cuts, for clarity of presentation, are indicated by dotted lines. All quantified data are presented as mean $\pm$ S.D. Comparisons between groups were made by Student's *t* test or with one-way ANOVA and Tukey's post hoc test as appropriate. $p < 0.05$ was considered significant.

Author Contributions—N. A. designed, performed, and analyzed the experiments. D. T. H. designed the experiments. P. J. M. performed the experiments. N. A., D. T. H., and J. S. S. wrote the paper.

Acknowledgments—We thank Robert J. Lefkowitz for providing HEK cell lines, Richard B. Clark for providing phospho-β_2AR antibody, and Masaki Fukuta for providing HA-zDHHC plasmids.

References

1. Qanbar, R., and Bouvier, M. (2003) Role of palmitoylation/depalmitoylation reactions in G-protein-coupled receptor function. *Pharmacol. Ther.* **97,** 1–33
2. O'Brien, P. J., and Zatz, M. (1984) Acylation of bovine rhodopsin by [^{3}H]palmitic acid. *J. Biol. Chem.* **259,** 5054–5057
3. O'Dowd, B. F., Hnatowich, M., Caron, M. G., Lefkowitz, R. J., and Bouvier, M. (1989) Palmitoylation of the human β_2-adrenergic receptor: mutation of Cys-341 in the carboxyl tail leads to an uncoupled nonpalmitoylated form of the receptor. *J. Biol. Chem.* **264,** 7564–7569
4. Loisel, T. P., Adam, L., Hebert, T. E., and Bouvier, M. (1996) Agonist stimulation increases the turnover rate of β_2AR-bound palmitate and promotes receptor depalmitoylation. *Biochemistry* **35,** 15923–15932
5. Liu, R., Wang, D., Shi, Q., Fu, Q., Hizon, S., and Xiang, Y. K. (2012) Palmitoylation regulates intracellular trafficking of β_2 adrenergic receptor/arrestin/phosphodiesterase 4D complexes in cardiomyocytes. *PLoS One* **7,** e42658
6. Forrester, M. T., Hess, D. T., Thompson, J. W., Hultman, R., Moseley, M. A., Stamler, J. S., and Casey, P. J. (2011) Site-specific analysis of protein *S*-acylation by resin-assisted capture. *J. Lipid Res.* **52,** 393–398
7. Forrester, M. T., Thompson, J. W., Foster, M. W., Nogueira, L., Moseley, M. A., and Stamler, J. S. (2009) Proteomic analysis of *S*-nitrosylation and denitrosylation by resin-assisted capture. *Nat. Biotechnol.* **27,** 557–559
8. Shenoy, S. K., McDonald, P. H., Kohout, T. A., and Lefkowitz, R. J. (2001) Regulation of receptor fate by ubiquitination of activated β_2-adrenergic receptor and β-arrestin. *Science* **294,** 1307–1313
9. Hannoush, R. N., and Arenas-Ramirez, N. (2009) Imaging the lipidome: ω-alkynyl fatty acids for detection and cellular visualization of lipid-modified proteins. *ACS Chem. Biol.* **4,** 581–587
10. Martin, B. R., and Cravatt, B. F. (2009) Large-scale profiling of protein palmitoylation in mammalian cells. *Nat. Methods* **6,** 135–138
11. Yap, M. C., Kostiuk, M. A., Martin, D. D., Perinpanayagam, M. A., Hak, P. G., Siddam, A., Majjigapu, J. R., Rajaiah, G., Keller, B. O., Prescher, J. A.,

Wu, P., Bertozzi, C. R., Falck, J. R., and Berthiaume, L. G. (2010) Rapid and selective detection of fatty acylated proteins using ω-alkynyl-fatty acids and click chemistry. *J. Lipid Res.* **51,** 1566–1580
12. Fukata, M., Fukata, Y., Adesnik, H., Nicoll, R. A., and Bredt, D. S. (2004) Identification of PSD-95 palmitoylating enzymes. *Neuron* **44,** 987–996
13. Tsutsumi, R., Fukata, Y., and Fukata, M. (2008) Discovery of protein-palmitoylating enzymes. *Pflugers Arch.* **456,** 1199–1206
14. Camp, L. A., and Hofmann, S. L. (1993) Purification and properties of a palmitoyl-protein thioesterase that cleaves palmitate from H-Ras. *J. Biol. Chem.* **268,** 22566–22574
15. Camp, L. A., Verkruyse, L. A., Afendis, S. J., Slaughter, C. A., and Hofmann, S. L. (1994) Molecular cloning and expression of palmitoyl-protein thioesterase. *J. Biol. Chem.* **269,** 23212–23219
16. Soyombo, A. A., and Hofmann, S. L. (1997) Molecular cloning and expression of palmitoyl-protein thioesterase 2 (PPT2), a homolog of lysosomal palmitoyl-protein thioesterase with a distinct substrate specificity. *J. Biol. Chem.* **272,** 27456–27463
17. Duncan, J. A., and Gilman, A. G. (1998) A cytoplasmic acyl-protein thioesterase that removes palmitate from G protein alpha subunits and $p21^{RAS}$. *J. Biol. Chem.* **273,** 15830–15837
18. Tomatis, V. M., Trenchi, A., Gomez, G. A., and Daniotti, J. L. (2010) Acyl-protein thioesterase 2 catalyzes the deacylation of peripheral membrane-associated GAP-43. *PLoS One* **5,** e15045
19. Davda, D., and Martin, B. R. (2014) Acyl protein thioesterase inhibitors as probes of dynamic *S*-palmitoylation. *Medchemcomm* **5,** 268–276
20. Lin, D. T., and Conibear, E. (2015) ABHD17 proteins are novel protein depalmitoylases that regulate N-Ras palmitate turnover and subcellular localization. *eLife* **4,** e11306
21. Ohno, Y., Kihara, A., Sano, T., and Igarashi, Y. (2006) Intracellular localization and tissue-specific distribution of human and yeast DHHC cysteine-rich domain-containing proteins. *Biochim. Biophys. Acta* **1761,** 474–483
22. Swarthout, J. T., Lobo, S., Farh, L., Croke, M. R., Greentree, W. K., Deschenes, R. J., and Linder, M. E. (2005) DHHC9 and GCP16 constitute a human protein fatty acyltransferase with specificity for H- and N-Ras. *J. Biol. Chem.* **280,** 31141–31148
23. Moore, C. A., Milano, S. K., and Benovic, J. L. (2007) Regulation of receptor trafficking by GRKs and arrestins. *Annu. Rev. Physiol.* **69,** 451–482
24. Hausdorff, W. P., Bouvier, M., O'Dowd, B. F., Irons, G. P., Caron, M. G., and Lefkowitz, R. J. (1989) Phosphorylation sites on two domains of the β_2-adrenergic receptor are involved in distinct pathways of receptor desensitization. *J. Biol. Chem.* **264,** 12657–12665
25. Zamah, A. M., Delahunty, M., Luttrell, L. M., and Lefkowitz, R. J. (2002) Protein kinase A-mediated phosphorylation of the β_2-adrenergic receptor regulates its coupling to G_s and G_i: demonstration in a reconstituted system. *J. Biol. Chem.* **277,** 31249–31256
26. Moffett, S., Adam, L., Bonin, H., Loisel, T. P., Bouvier, M., and Mouillac, B. (1996) Palmitoylated cysteine 341 modulates phosphorylation of the β_2-adrenergic receptor by the cAMP-dependent protein kinase. *J. Biol. Chem.* **271,** 21490–21497
27. Tran, T. M., Friedman, J., Qunaibi, E., Baameur, F., Moore, R. H., and Clark, R. B. (2004) Characterization of agonist stimulation of cAMP-dependent protein kinase and G protein-coupled receptor kinase phosphorylation of the β_2-adrenergic receptor using phosphoserine-specific antibodies. *Mol. Pharmacol.* **65,** 196–206
28. Nobles, K. N., Xiao, K., Ahn, S., Shukla, A. K., Lam, C. M., Rajagopal, S., Strachan, R. T., Huang, T. Y., Bressler, E. A., Hara, M. R., Shenoy, S. K., Gygi, S. P., and Lefkowitz, R. J. (2011) Distinct phosphorylation sites on the β_2-adrenergic receptor establish a barcode that encodes differential functions of β-arrestin. *Sci. Signal.* **4,** ra51
29. January, B., Seibold, A., Whaley, B., Hipkin, R. W., Lin, D., Schonbrunn, A., Barber, R., and Clark, R. B. (1997) β_2-adrenergic receptor desensitization, internalization, and phosphorylation in response to full and partial agonists. *J. Biol. Chem.* **272,** 23871–23879
30. Reiner, S., Ambrosio, M., Hoffmann, C., and Lohse, M. J. (2010) Differential signaling of the endogenous agonists at the β_2-adrenergic receptor. *J. Biol. Chem.* **285,** 36188–36198
31. Wisler, J. W., DeWire, S. M., Whalen, E. J., Violin, J. D., Drake, M. T., Ahn, S., Shenoy, S. K., and Lefkowitz, R. J. (2007) A unique mechanism of β-blocker action: carvedilol stimulates β-arrestin signaling. *Proc. Natl. Acad. Sci. U.S.A.* **104,** 16657–16662
32. Shenoy, S. K., and Lefkowitz, R. J. (2011) β-Arrestin-mediated receptor trafficking and signal transduction. *Trends Pharmacol. Sci.* **32,** 521–533
33. Rasmussen, S. G., Choi, H. J., Rosenbaum, D. M., Kobilka, T. S., Thian, F. S., Edwards, P. C., Burghammer, M., Ratnala, V. R., Sanishvili, R., Fischetti, R. F., Schertler, G. F., Weis, W. I., and Kobilka, B. K. (2007) Crystal structure of the human β_2 adrenergic G-protein-coupled receptor. *Nature* **450,** 383–387
34. Shenoy, S. K., Drake, M. T., Nelson, C. D., Houtz, D. A., Xiao, K., Madabushi, S., Reiter, E., Premont, R. T., Lichtarge, O., and Lefkowitz, R. J. (2006) β-arrestin-dependent, G protein-independent ERK1/2 activation by the β_2 adrenergic receptor. *J. Biol. Chem.* **281,** 1261–1273
35. Zuckerman, D. M., Hicks, S. W., Charron, G., Hang, H. C., and Machamer, C. E. (2011) Differential regulation of two palmitoylation sites in the cytoplasmic tail of the β_1-adrenergic receptor. *J. Biol. Chem.* **286,** 19014–19023
36. Hancock, J. F., Magee, A. I., Childs, J. E., and Marshall, C. J. (1989) All Ras proteins are polyisoprenylated but only some are palmitoylated. *Cell* **57,** 1167–1177
37. Jeong, W. J., Yoon, J., Park, J. C., Lee, S. H., Lee, S. H., Kaduwal, S., Kim, H., Yoon, J. B., and Choi, K. Y. (2012) Ras stabilization through aberrant activation of Wnt/β-catenin signaling promotes intestinal tumorigenesis. *Sci. Signal.* **5,** ra30
38. Devic, E., Xiang, Y., Gould, D., and Kobilka, B. (2001) β-adrenergic receptor subtype-specific signaling in cardiac myocytes from β_1 and β_2 adrenoceptor knockout mice. *Mol. Pharmacol.* **60,** 577–583
39. Steinberg, S. F. (2004) β_2-Adrenergic receptor signaling complexes in cardiomyocyte caveolae/lipid rafts. *J. Mol. Cell. Cardiol.* **37,** 407–415
40. Lorent, J. H., and Levental, I. (2015) Structural determinants of protein partitioning into ordered membrane domains and lipid rafts. *Chem. Phys. Lipids* **192,** 23–32
41. Galbiati, F., Volonte, D., Meani, D., Milligan, G., Lublin, D. M., Lisanti, M. P., and Parenti, M. (1999) The dually acylated NH_2-terminal domain of $G_{i1\alpha}$ is sufficient to target a green fluorescent protein reporter to caveolin-enriched plasma membrane domains: palmitoylation of caveolin-1 is required for the recognition of dually acylated G-protein α subunits *in vivo*. *J. Biol. Chem.* **274,** 5843–5850
42. Chen, C. A., and Manning, D. R. (2001) Regulation of G proteins by covalent modification. *Oncogene* **20,** 1643–1652
43. Ballesteros, J. A., Jensen, A. D., Liapakis, G., Rasmussen, S. G., Shi, L., Gether, U., and Javitch, J. A. (2001) Activation of the β_2-adrenergic receptor involves disruption of an ionic lock between the cytoplasmic ends of transmembrane segments 3 and 6. *J. Biol. Chem.* **276,** 29171–29177
44. Shukla, A. K., Sun, J. P., and Lefkowitz, R. J. (2008) Crystallizing thinking about the β_2-adrenergic receptor. *Mol. Pharmacol.* **73,** 1333–1338
45. Muntz, K. H., Zhao, M., and Miller, J. C. (1994) Downregulation of myocardial β-adrenergic receptors: receptor subtype selectivity. *Circ. Res.* **74,** 369–375
46. Wilmore, D. W., Long, J. M., Mason, A. D., Jr, Skreen, R. W., and Pruitt, B. A., Jr. (1974) Catecholamines: mediator of the hypermetabolic response to thermal injury. *Ann. Surg.* **180,** 653–669
47. Irannejad, R., Tomshine, J. C., Tomshine, J. R., Chevalier, M., Mahoney, J. P., Steyaert, J., Rasmussen, S. G., Sunahara, R. K., El-Samad, H., Huang, B., and von Zastrow, M. (2013) Conformational biosensors reveal GPCR signalling from endosomes. *Nature* **495,** 534–538
48. Iwakiri, Y., Satoh, A., Chatterjee, S., Toomre, D. K., Chalouni, C. M., Fulton, D., Groszmann, R. J., Shah, V. H., and Sessa, W. C. (2006) Nitric oxide synthase generates nitric oxide locally to regulate compartmentalized protein *S*-nitrosylation and protein trafficking. *Proc. Natl. Acad. Sci. U.S.A.* **103,** 19777–19782
49. Ozawa, K., Whalen, E. J., Nelson, C. D., Mu, Y., Hess, D. T., Lefkowitz, R. J., and Stamler, J. S. (2008) *S*-Nitrosylation of β-arrestin regulates β-adrenergic receptor trafficking. *Mol. Cell* **31,** 395–405